Spring 5-2020

The Role of the BPs Immunity Repressor in the Regulation of Pathogenic Mycobacterium chelonae Gene Expression

Emma Freeman

THE ROLE OF THE BPS IMMUNITY REPRESSOR IN THE REGULATION OF PATHOGENIC *MYCOBACTERIUM CHELONAE* GENE EXPRESSION

by

Emma Freeman

A Thesis Submitted in Partial Fulfillment
of the Requirements for a Degree with Honors
(Microbiology)

The Honors College

University of Maine

May 2020

Advisory Committee:
Sally Molloy, Assistant Professor of Genomics, Advisor
Edward Bernard, Lecturer & Undergraduate Coordinator, Molecular and Biomedical Sciences
Keith Hutchison, Professor Emeritus, Molecular and Biomedical Sciences
Melody Neely, Associate Professor, Molecular and Biomedical Sciences
Sharon Tisher, Lecturer, School of Economics and Honors College

ABSTRACT

Mycobacterium tuberculosis is the leading cause of death by an infectious disease (MacNeil, 2019). In 2018, 10 million people developed tuberculosis and half a million infections were resistant to antibiotics (WHO, 2019). Nearly all members of the *M. tuberculosis* complex are lysogens, meaning they carry prophage, or integrated viral genomes within the host genome (Fan et al., 2016). The non-pathogenic vaccine strain (*M. bovis* Bacillus Calmette–Guérin (BCG)) is the exception, which suggests prophage play a role in virulence (Fan et al., 2016). Because not all prophage encode obvious virulence genes, we hypothesize that prophage impact bacterial virulence by altering bacterial gene expression. By studying gene expression patterns in *M. chelonae*, a close relative of *M. tuberculosis*, in the presence and absence of prophage BPs, we determined prophage impact mycobacterial gene expression. Through RNAseq analysis of *M. chelonae* with or without prophage, we detected significant changes in expression of almost 8% of *M. chelonae* genes, including the gene *whi*B7, which is involved in antibiotic resistance. During lysogenic infection of *M. chelonae* the most highly expressed gene from the BPs prophage was the immunity repressor (gp33). To determine if viral gene products drive changes in expression of *whi*B7, strains of *M. chelonae* that express gp33 were created and gene expression and antibiotic resistance analyses were performed. Expression of gp33 did not alter expression of *M. chelonae whi*B7 nor antibiotic resistance. We are now investigating alternative hypotheses to explain how prophage alter *whi*B7 expression.

ACKNOWLEDGEMENTS

I would like to say thank you to Dr. Sally Molloy for her guidance, support, and encouragement over the past four years, both in and out of the lab. I would like to thank Dr. Keith Hutchison for his words of wisdom and commitment to this thesis project and my own personal goals. I would like to say a special thank you to Jaycee Cushman for never allowing me to doubt myself and always offering words of advice that do not just apply to the lab. I would like to thank the members of my advisory committee: Dr. Edward Bernard, Dr. Melody Neely, and Sharon Tisher for their commitment to this thesis project and flexibility. The following members of the Molloy Lab have all contributed to this project: Sarah McCallister, Dakota Archambault, Anna Schumann, Colin Welch, Jacob Cote, Maddie Kimble, Matthew Cox, and Caitlin Selassie Naa Sar Wiafe-Kwakye. The following departments have supported our research: The University of Maine Honors College, the Department of Molecular and Biomedical Sciences, and Dr. Graham Hatfull and the SEA-PHAGES program.

I would like to thank the following sources of funding: the INBRE Junior Year Research Award and Comparative Functional Genomics Thesis Fellowship, the INBRE Senior Year Research Award and Comparative Functional Genomics Thesis Fellowship, the Charlie Slavin Research Fund, the Department of Molecular and Biomedical Sciences Frederick Radke Fund. Lastly, Research reported in this project was supported by an Institutional Development Award (IDeA) from the National Institute of General Medical Sciences of the National Institutes of Health under grant number P20GM103423.

TABLE OF CONTENTS

LIST OF FIGURES

LIST OF TABLES

INTRODUCTION

Mycobacterium tuberculosis is one of the top ten leading causes of death globally (WHO, 2019) and is the leading cause of death by an infectious disease (MacNeil, 2019). In 2018, 10 million new cases of tuberculosis were diagnosed and 500,000 cases were deemed multidrug resistant (MDR) (WHO, 2019). Non-tuberculosis mycobacteria are becoming increasingly drug-resistant and there is a need for alternative therapeutics. *M. abscessus*, for example, is an emerging pathogen in cystic fibrosis patients, and is extremely difficult to treat as some isolates are completely resistant to available antibiotics (Bryant et al., 2013). In order to develop new treatments for pathogens such as *M. tuberculosis* and *M. abscessus*, we must understand their mechanisms of pathogenicity and virulence. One aspect of mycobacterial pathogenicity that is not well understood is the role of prophage.

Bacteriophage (phage) are viruses that infect bacteria, while prophage are phage genomes that have integrated into bacterial genomes, creating a bacterial cell called a lysogen (Hatfull, 2011). The lysogenic state is established and maintained via the expression of the prophage-encoded immunity repressor protein (Shimatake, H., Rosenberg, M., 1981). The repressor binds to specific DNA sequences within the phage genome to prevent transcription of phage lytic genes during lysogeny, and can bind to invading genomes of similar phage to confer superinfection immunity to its bacterial host (Brussow et al., 2004). Prophage may express additional genes that contribute to virulence and pathogenicity of the bacterial host. For example, *Escherichia coli* O157:H7 only causes illness when a Shiga-like toxin is expressed from a prophage (Fang et al., 2017).

However, not all prophage encode obvious virulence factors. The virulent *M. tuberculosis* strain H37Rv carries two prophage, while the nonvirulent vaccine strain *M. bovis* BCG does not carry prophage (Fan et al., 2016). It is hypothesized the prophage impact the pathogenicity of their mycobacterial hosts, but how they do so is still unknown (Fan et al., 2016). Given that there are no obvious virulence factors encoded by the prophage, it's possible that prophage alter expression of bacterial virulence genes.

The Molloy lab has determined that the prophage, BPs, significantly alters gene expression and antibiotic resistance of the non-tuberculosis mycobacterial pathogen, *M. chelonae* (Sampson et al., 2009). The presence of the BPs prophage causes differential expression of 7% of *M. chelonae* genes (Molloy, unpublished). Genes associated with antibiotic resistance, *whi*B7 and a *pad*R-like transcription factor (referred to as *pad*R), were significantly up- and down-regulated, respectively. WhiB7 is a transcription factor that upregulates a regulon of genes, many of which impact antibiotic resistance, and are conserved in all mycobacteria, including *M. tuberculosis* and *M. abscessus* (Burian et al., 2012, Hess et al., 2017). PadR is a transcriptional regulator that negatively regulates genes that function in responding to environmental stressors, such as antibiotics or phenolic acid, and is itself down regulated upon cellular exposure to antibiotics or other toxic compounds (Park et al., 2017). The changes in *whi*B7 and *pad*R expression may explain the increased resistance to antibiotics observed in BPs-*M. chelonae* lysogens relative to *M. chelonae* Wild-Type (WT). The BPs-*M. chelonae* lysogen has increased viability in the presence of antibiotics compared to that of the non-BPs lysogen, *M. chelonae* WT. It is not understood how the presence of BPs alters expression of *whi*B7 and *pad*R. It is possible that genes expressed from the prophage genome, such as the immunity repressor, gp33, drive changes

in bacterial gene expression. The most highly expressed prophage-encoded gene during lysogenic infection of *M. chelonae* is the BPs immunity repressor, gp33 (Molloy, unpublished). If BPs gp33 is responsible for the changes we see in gene expression and antibiotic resistance during BPs lysogenic infection of *M. chelonae*, we should see similar changes in gene expression and antibiotic resistance profiles in a strain of *M. chelonae* expressing only BPs gp33 as observed in the BPs-*M. chelonae* lysogen.

The goal of this project was to create a recombinant strain *M. chelonae* (pMHIR), that expresses the BPs immunity repressor, gp33, to determine if it is responsible for the changes in bacterial gene expression and antibiotic resistance observed in the BPs-*M. chelonae* lysogen. Using an integrative vector, control and experimental recombinant strains of *M. chelonae* were constructed that express the BPs integrase alone or with a functional BPs immunity repressor. Integration of the plasmids into the bacterial genome was detected by PCR analysis and the ability of these strains to produce a functional repressor protein was tested by superinfection immunity assays. To measure the impact of repressor function on *pad*R and *whi*B7 expression in the experimental and control recombinant strains, RNA was isolated and analyzed by qRT-PCR. To determine if the immunity repressor increases *M. chelonae* antibiotic resistance, minimum inhibitory concentration (MIC) assays were conducted on the recombinant strains in the presence of clarithromycin and tetracycline, antibiotics commonly used to treat mycobacterial infections.

LITERATURE REVIEW

Pathogenic Mycobacteria

Actinobacteria are one of the largest bacterial phyla and include numerous pathogens. Bacteria belonging to the Actinobacteria phylum are Gram-positive and have high G/C content in their genomes, meaning a majority of their genome is made up of guanine and cytosine nucleotides as opposed to adenine and thymine. (Barka et al., 2015). They are found in soil, fresh and marine waters, and man-made water distribution systems (Percival, 2014). One of the most important genera within the Actinobacteria is *Mycobacterium*, a genus that contains multiple pathogens (Percival, 2014). Mycobacteria include both obligate and opportunistic pathogens that cause pulmonary diseases, skin lesions, and abscesses (Percival, 2014).

Mycobacteria cause more deaths worldwide than any other infectious agent (Bussi, 2019). *M. tuberculosis* alone causes approximately 1.5 million deaths and 10 million new infections every year (WHO, 2019). Tuberculosis causes a pulmonary infection and presents as chest pain and a chronic cough that may expel blood or sputum (Zaman, 2010). Latent (asymptomatic) tuberculosis infects 25% of the population (MacNeil, 2019). Non-tuberculosis mycobacteria (NTM) can also cause lung infections and account for 13% of lung infections in cystic fibrosis patients (Jones et al., 2019). Members of the *M. abscessus* complex cause skin and soft tissue infections, central nervous system infections, bacteremia, ocular infections and chronic respiratory disease (Lee et al., 2015). The *M. abscessus* complex is responsible for 80% of pulmonary infections caused by NTM (Daley, C. 2016). *M. abscessus* is an emerging pathogen in cystic fibrosis patients, and is extremely

difficult to treat as some isolates are completely resistant to available antibiotics (Bryant et al., 2013).

M. chelonae is an ideal model for studying the more dangerous mycobacterial pathogens, such as *M. abscessus* and *M. tuberculosis* as it is pathogenic in humans and has high intrinsic antibiotic resistance (McFee, 2013). *M. chelonae* can cause disseminated skin disease, including cellulitis and abscesses, and can be acquired from contaminated water or infected surgical implantations (McFee, 2013). Based on multiple conducted studies, infections caused by the *M. abscessus/M. chelonae* group account for 3–13% of all pulmonary infections caused by mycobacteria (Lee et al., 2015). *M. chelonae* and *M. abscessus* were considered the same species until 1992 because of their high sequence similarity (Lee et al., 2015). The overall prevalence of *M. abscessus/M. chelonae* infections is increasing, as is their ability to become multidrug resistant (Jones et al., 2019).

Prevalence of antibiotic resistant mycobacteria

The incidence of antibiotic resistant mycobacteria is increasing due to the heavy use of antibiotics to treat bacterial, including mycobacterial, infections. For example, in 2017, there were 10 million new cases of tuberculosis (MacNeil, 2019). Of all tuberculosis cases, 5.6% were deemed rifampicin resistant (RR) or multidrug-resistant (MDR), including 3.6% of new cases and 18% of previously diagnosed cases (MacNeil, 2019). Non-tuberculosis mycobacteria (NTM), including *M. abscessus* are resistant to almost all first-line drugs (Lee et al., 2015). The current treatment for *M. abscessus* infections includes a mix of the antibiotics clarithromycin, cefoxitin and amikacin, among others. However, amikacin resistance is growing, it is only about 50% effective, and has debilitating side effects (Hess et al., 2017). Understanding the underlying mechanisms of

how pathogenic mycobacteria are growing increasingly resistant to antibiotics is key to developing new therapeutics.

Mycobacteria have various intrinsic properties that confer antibiotic resistance and make them difficult to treat (Nyugen, L., Thompson, C. 2006). For example, mycobacteria are known for their selectively permeable cell wall with an internal waxy barrier that limits the diffusion of hydrophobic and hydrophilic molecules, including antimicrobial agents (Nyugen, L., Thompson, C. 2006). Mycobacteria also encode genes that provide intrinsic antibiotic resistance and their expression is upregulated in the presence of sub-inhibitory concentrations of antibiotics, such as aminoglycosides (Nyugen, L., Thompson, C. 2006). Aminoglycosides bind to the 16s rRNA of the 30S ribosomal subunit, therefore mutations in the 16s rRNA change the ability of aminoglycosides to bind to the 30S ribosome (Zaunbrecher et al. 2009). Genes that confer antibiotic resistance include: efflux pumps, which transport drugs out of the cell through ABC transporters and facilitator proteins; antibiotic modifying enzymes; antibiotic degrading enzymes, and target-modifying enzymes (Nyugen, L., Thompson, C. 2006). Many of these genes belong to the WhiB7 regulon, genes that are expressed in the presence of the transcription factor *whi*B7.

WhiB7 is an autoregulated transcriptional activator of resistance genes and belongs to the WhiB family of transcription factors that is conserved across Actinobacteria (Hess, 2017). Expression of *whi*B7 is dependent upon one promoter approximately 350 – 450-bp upstream of the *whi*B7 gene in mycobacteria (Burian, 2018). Between the promoter and upstream of the *whi*B7 gene there is an open reading frame (uORF) that does not encode a functional protein (Burian, 2018). The uORF rather serves as a means of regulating transcript elongation across a transcriptional terminator sequence that is positioned

between the uORF and the *whi*B7 ORF (Burian, 2018). Transcription of the *whi*B7 ORF increases in the intracellular environment of the macrophage and with sub-inhibitory concentrations of antibiotics including tetracycline, fluoroquinolones, macrolides, and aminoglycosides (Nyugen, L., Thompson, C. 2006). Genes under the *M. tuberculosis* and *M. abscessus* WhiB7 regulon include *erm*, *eis*, and the *tet*V efflux pump (Burian, 2018, Hess et al., 2017).

The Whib7 regulon in *M. tuberculosis* and *M. abscessus* includes a variety of genes that lead to resistance to aminoglycosides, macrolides, and tetracycline (Burian et al., 2012, Burian, 2018, Hess et al., 2017). *erm* is induced by macrolides, such as clarithromycin and azithromycin, and acts as a ribosomal RNA methyltransferase to prohibit macrolides from binding to sites in the 23S rRNA, thus preventing translation (Nyugen, 2006., Hess, 2017). *Eis* acetylates aminoglycosides, such as kanamycin and amikacin, which prevents the drugs from binding to the 30S rRNA subunit and inhibiting translation (Burian et al., 2012). *M. abscessus* contains two *eis* genes, both N-acetyl transferases, and *eis*2 is responsible for aminoglycoside resistance (Burian et al., 2012). Lastly, *tap* and *tet*V utilizes the proton motive force to work as an efflux pump to export aminoglycosides and tetracycline from the cytoplasm (Burian et al., 2012 (B)). Mechanisms of regulation of these antibiotic resistance genes are fairly well studied (Burian et al., 2012, Burian et al., 2012 (B), Burian, 2018, Hess et al, 2017). Prophage are known to alter antibiotic resistance in some bacteria, but their role in regulating antibiotic resistance genes has not been studied (Wang et al., 2010).

Bacteriophage and Prophage Characteristics

Bacteriophage (phage), viruses that infect bacteria, are the most abundant biological entity with an estimated 10^{31} particles in the world (Hendrix, 2003). Viruses that infect bacteria of the genus *Mycobacterium* are termed mycobacteriophage and this population appears to also be incredibly abundant and incredibly diverse (Hatfull, 2014, Jacobs-Sera et a., 2012, Pope et al., 2011). To understand the relationships and evolution of phage, they are organized into clusters based on genome sequence identity and shared gene content (Pope et al., 2017). As of April 26th, 2020, there are 1,885 sequenced mycobacteriophage genomes belonging to 29 different clusters, 30 including singletons (Russell D., Hatfull, G. 2017). Some clusters of phage are well characterized and include clusters A, G, K, M, N, and O (Cresawn et al., 2015., Caratenuto et al., 2019., Sampson et al., 2009).

Cluster G mycobacteriophage include 73 members that typically can infect multiple species of *Mycobacterium* including *M. tuberculosis*, *M. smegmatis*, *M. abscessus* and *M. chelonae* (PhagesDB, Jacobs-Sera, 2012; Molloy unpublished). The cluster includes members BPs, CLED96, Angel and Halo (Sampson et al., 2009; Russel et al., 2017). Cluster G phage are temperate, meaning they can carry out one of two growth cycles: the lytic or lysogenic cycle (Sampson et al., 2009). In the lytic pathway, phage genomes are replicated and packaged into new phage particles, which are released by lysis of the bacterial cell (Hatfull, 2011). During lysogenic growth, the phage genome is integrated into the host genome via a phage-encoded protein called the integrase (Hatfull, 2011). The integrated phage genome is called a prophage and it is replicated each time the bacterial cell replicates (Hatfull, 2011).

Understanding the organization of cluster G genomes allows for further understanding of their lysogenic regulation. The genomes of cluster G mycobacteriophage are relatively small at around 40 kbp and organized into a left arm of rightward-transcribed genes and a right arm of leftward and rightward transcribed genes (Figure 1) (Sampon et al., 2009). The left arm contains genes involved in particle structure and assembly, including one operon which encodes the structural genes, terminase, portal protein, capsid maturation protease, and gp5 (Sampson et al., 2009). gp5 is a small gene of unknown function, but has strong HHpred matches to the ribosome modulation factor of *Escherichia coli* (Zimmermann et al., 2018). The right arm encodes genes that are predicted to be involved in the early lytic cycle, but the majority of genes have no known function (Sampson et al., 2009). Some cluster G genomes, including BPs, contain a *Mycobacterium* phage mobile element (MPME) in their right arm (Sampson et al., 2009). The function of the gene within the MPME (gp58 in the BPs genome) is not known, but presumed to be a transposase (Sampson et a., 2009). The left and right arm are separated by an integration cassette, which encodes an integrase gene and transcriptional regulators, the immunity repressor and Cro-like protein, that regulate genes involved in lytic versus lysogenic growth (Sampson et al., 2009).

Phage use various mechanisms to establish and maintain lysogeny, including proteins expressed from an integration cassette. Temperate phage that do not have an integration cassette utilize a plasmid-like partitioning system that allows them to partition episomal phage genomes into dividing cells (Dedrick et al., 2016). Most temperate phage maintain lysogeny by integrating the phage genome into that of the host (Hatfull, 2011). This requires a phage-encoded integrase cassette that includes an integrase and an

immunity repressor protein that represses lytic gene expression (Hatfull, et al., 2011). During lysogeny, the bacterial cell containing the phage genome is termed a *lysogen*, while the integrated phage genome is termed a *prophage* (Hatfull, 2011). In the Cluster G phage, the integrase and repressor establish lysogeny in an integration-dependent manner (Sampson et al., 2009).

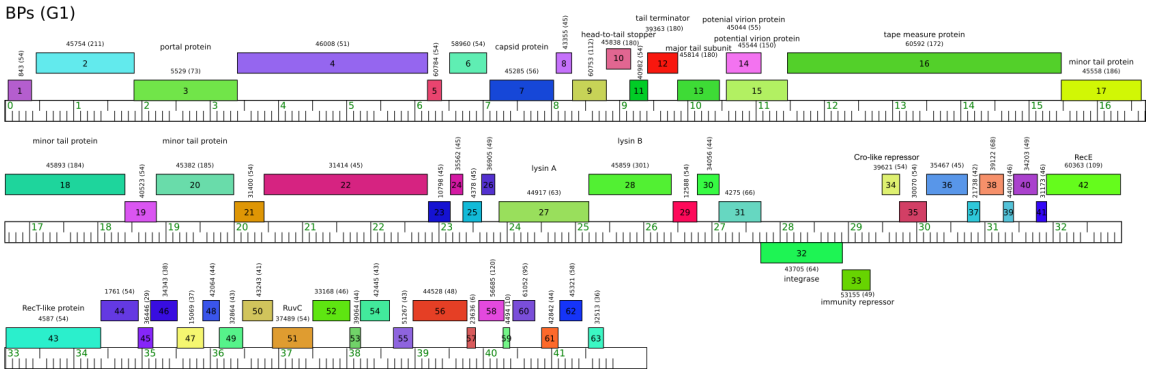

Figure 1. Genome map of BPs drawn to scale with the ruler indicating the coordinates of the genome in units of kilobasepairs (Kbp) (Cresawn et al., 2011). Genes transcribed rightwards are positioned above the ruler and genes transcribed leftwards are positioned below the ruler. Genes are color coded based on similarity with other genes in the Phamerator database.

Phage Integrases

Phage integrases utilize a site-specific mechanism to mediate integration into the host cell (Groth et al., 2004). Recombination occurs via a tyrosine or serine integrase, which initiate attack of the DNA sugar-phosphate backbone at two sites of recombination in the phage genome, called the phage attachment site (*att*P), and the bacterial attachment site (*att*B) in the bacterial genome (Groth et al., 2004). Most phage utilize a tyrosine integrase, which recognize larger core attachment sites, 30 – 40 bp in length, with an inverted recognition sequence region (Groth et al., 2004). Recombination occurs when a nucleophilic tyrosine nicks one strand of each *att* site, resulting in the formation of a Holliday junction (Holliday, 1964, Grindley et al., 2006). The Holliday junction eventually

resolves and the resulting *att*L (left) and *att*R (right) sites are hybrid sequences of the *att*P and *att*B sites, leaving the prophage sequence flanked by the *att*L and *att*R sites (Groth et al., 2004). The new prophage state is maintained via expression of the prophage-encoded repressor (Petrova, 2015).

Phage Repressors

The most highly expressed gene during lysogenic infection is typically the repressor and its function is to prevent lytic genes from being transcribed to maintain the lysogenic state (Petrova, 2015). The most well-studied repressor system is that of the temperate *E. coli* phage, Lambda (ƛ) (Gao et al., 2013). The ƛ immunity cassette contains genes that encode transcriptional regulators CI, CII, and Cro (Figure 2). CI and CII expression promotes lysogenic growth and Cro expression promotes lytic growth (Atsumi, 2006). CI and Cro are divergently transcribed and there are three operator sequences that overlap the promoters for these genes (Atsumi, 2006). From right to left the operator sites are termed O_R3, O_R2 and O_R1. The CI protein acts as a repressor for lytic genes by binding to O_R1 and O_R2 upstream of the promoter P_R, thus prohibiting the polymerase from binding the rightward promoter and transcribing lytic genes, including Cro (Atsumi, 2006). Cro will bind to O_R3 and O_R2 upstream of the leftward promoter P_{RM}. Binding of Cro prevents transcription of CI, while allowing transcription from P_R and expression of lytic genes (Atsumi, 2006).

The lytic/lysogenic decision is dependent upon levels of the CII transcriptional activator that promotes transcription of integrase (from P_I) and of CI from the repressor establishment promoter (P_{RE}) (Rokney et al., 2008). The stability of the CII protein determines its ability to stimulate transcription of those genes (Rokney et al., 2008). When

the nutrient status of the cell is high, HflA protease complex levels are high, and CII is degraded by the HflA protease complex. This allows accumulation of Cro in the cells, transcription from P_R, and the cells will undergo the lytic cycle (Rokney et al., 2008). When nutrient levels in the cell are low, HflA protease complex levels are low, and CII is not degraded by the HflA protease complex, allowing establishment of CI in the cells. This allows continued transcription from P_{RM}, and the phage undergoes the lysogenic growth cycle (Figure 2) (Rokney et al., 2008). Phage repressors, such as CI, can also bind to the genomes of similar superinfecting phage and prohibit lytic gene expression, thus conferring superinfection immunity (Sampson et al., 2009). Although the Lambda model is the most well-studied, CI/Cro systems have been found in many prophage, including those belonging to Cluster N and Cluster G (Dedrick et al., 2017., Broussard et al., 2013).

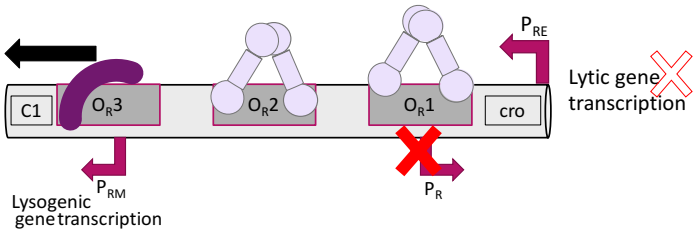

Figure 2. Model of Lambda repressor expression. Upon integration, dimers of the lysogenic repressor protein, CI (light purple), will bind to O_R1 and O_R2, prohibiting transcription of the lytic repressor, Cro, from the lytic promoter, P_R. The RNA polymerase is recruited to the lysogenic promoter, P_{RM}, and CI is continuously expressed.

BPs Maintenance of Lysogeny

BPs is a temperate, Cluster G phage (Sampson et al., 2009). It has a broad host range capable of infecting *M. smegmatis*, *M. abscessus*, *M. chelonae*, and *M. tuberculosis* (Illingworth, unpublished, Jacobs-Sera et al., 2012, Dedrick et al., 2019 (B)). BPs infects *M. smegmatis* with an efficiency of lysogeny of 5% and *M. chelonae* WT with an efficiency of lysogeny of 25% (Jacobs-Sera et al., 2012, Molloy, unpublished). BPs can infect *M. tuberculosis* with a reduced efficiency of lysogeny when there is a single amino acid

substitution in one of its tail fibers (Jacobs-Sera et al., 2012). Upon infection, the BPs genome integrates into the host genome where it is maintained as a prophage (Broussard et al., 2013). The BPs repressor functions only upon integration of the BPs genome into that of its bacterial host (Broussard et al., 2013).

Bps Integration Cassette and Integration-Dependent Immunity

BPs encodes an unusual integrase and immunity cassette in that the *att*P site is located within the 3′ end of the repressor (Broussard et al., 2013). The linear BPs genome is separated by an integration cassette that encodes a tyrosine integrase, a leftward-oriented immunity repressor (gp33) a rightward transcribed Cro (gp34), and an *att*P located within the 3′ end of the repressor (Figure 3). Upon integration at the *att*P site, the repressor is truncated (Broussard et al., 2013). Truncation of the repressor gene results in synthesis of a repressor protein that lacks the C-terminus, which includes ssrA-like tag (Broussard et al., 2013). This sequence is recognized and targets the protein for degradation by ClpXP or ClpAP proteases (Broussard et al., 2013). Removal of the 3′ end of the repressor gene upon integration therefore allows expression of a stable repressor protein that will repress transcription of lytic genes and promote the lysogenic lifestyle in a manner similar to phage ƛ (Broussard et al., 2013).

The main role of gp33 is to repress the expression from lytic gene promoters, including promoter P_R. The binding sites (called operators) for the active repressor consist of a 12-bp palindrome sequence of 5′-CGACATATGTCG-3′ (Villanueva, 2015). The operator upstream of P_R is termed O_R, while the operator upstream of the lysogenic promoter P_{Rep} is termed O_{Rep}. The active repressor $gp33^{103}$ (truncated prophage version) will bind to the operator site O_R, thus prohibiting RNA polymerase from binding and transcribing lytic

genes, including Cro (Villanueva, 2015). Expression of the repressor from the promoter P_{Rep} maintains the prophage in the lysogen, while conferring superinfection immunity to the host. Now that the prophage is integrated into the lysogen, its survival is dependent on that of its host. Many prophage have evolved to contribute to host fitness and pathogenesis (Brussow et al., 2004).

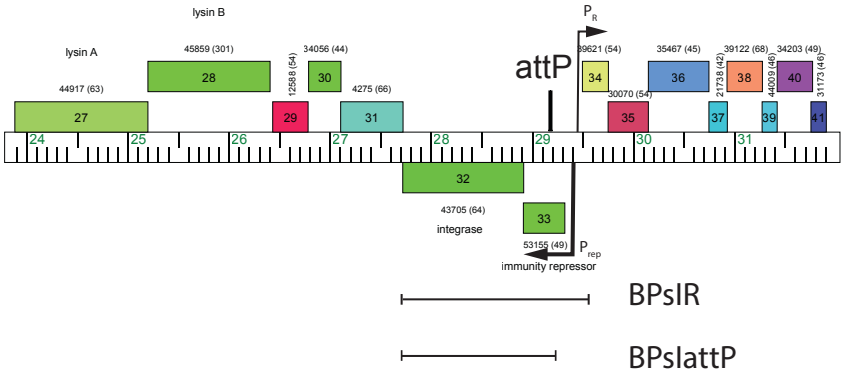

Figure 3. BPs integration cassette. The lysogenic promoter, P_{Rep}, and lytic promoter, P_R, are indicated by black arrows, showing the direction of transcription of the immunity repressor (gp33) and Cro-like protein (gp34), respectively. The phage attachment site (*att*P) is located with the BPs repressor gene, gp33. Cloning inserts BPsIR and BPsIattP were amplified from the BPs genome are indicated below the genome map. Insert BPsIR encodes the P_{rep}, the immunity repressor (gp33), *att*P site, and the integrase (gp32). Insert BPsIattP encodes the integrase (gp32), attP site, and 221-bp upstream of the *att*P site.

Role of Prophage in Mycobacterial Disease

Almost all pathogenic bacteria carry prophage in their genomes and prophage are known to impact host fitness in a variety of ways (Brussow et al., 2004). Prophage rearrangements can be beneficial for the host, they can disrupt host genes, protect their host from lytic infection by similar phage (superinfection immunity) and they can introduce genes that increase the virulence of the host (Brussow et al., 2004). Some prophage do so by encoding obvious virulence factors. In the example of Stx-producing *Escherichia coli* (STEC), a Shiga-like toxin is encoded by the prophage and *E. coli* only produces illness when the Shiga-like toxin is present (Fang et al., 2017). Both *Corynebacterium diphtheriae* and *Clostridium botulinum* are also infected with phage that encode toxin factors (Wang,

2010). However, not all prophage encode obvious virulence factors. This is the case for the phiRv1 and phiRv2 prophage of *M. tuberculosis*. For example, most strains of the *M. tuberculosis* complex (MTBC) carry the prophage phiRv1or phiRv2 (Fan et al., 2016). The prophage genes were upregulated in a nutrient starvation model of *M. tuberculosis* in the presence of oxidative phosphorylation inhibitors (ie: Valinomycin), and in the presence of metabolism inhibitors (ie: hypoxic conditions) (Fan et al., 2016). While the most virulent strain *M. tuberculosis* H37Rv carries both, the non-virulent strain *M. bovis* (BCG) does not carry phiRv1 nor phiRv2. This leads to the hypothesis that prophage are responding to changes in their host's environment and somehow impacting host virulence.

The presence of the prophage BPs alters expression of 7.7% of the bacterial genes associated with virulence and antibiotic resistance in *M. tuberculosis* (Molloy, unpublished, Burian et al., 2012). One gene that is significantly upregulated in the BPs-*M. chelonae* lysogen is the transcription factor *whi*B7, which regulates transcription of genes involved in antibiotic resistance (Burian et al., 2012, Burian, 2018). Since many genes involved in antibiotic resistance belong to the WhiB7 regulon, increased levels of *whi*B7 expression should lead to increased levels of antibiotic resistance. Compared to *M. chelonae* WT, BPs-*M. chelonae* lysogens are more resistant to aminoglycosides (kanamycin and amikacin) and tetracycline, antibiotics commonly used to treat *M. abscessus* and *M. tuberculosis* infections (Molloy, unpublished). The second most downregulated gene in the lysogen is a padR-like gene that may also be involved in antibiotic resistance. The first PadR transcription factor described in bacteria is a negative controller of phenolic acid decarboxylase, which detoxifies harmful phenolic acids (Park et al., 2017). In other bacterial species, PadR-like transcriptional regulators control

expression of stress response genes including multidrug efflux pumps, and transmembrane proteins that respond to stressors on the cell envelope (Hauf et al., 2019, Fibriansah et al., 2012, Vatlin et al., 2018). PadR family of transcriptional regulators are typically downregulated in the presence of environmental stressors, such as antibiotics, allowing de-repression of genes needed to survive the environmental stress (Park et al., 2017). The presence of a prophage in the mycobacterial host, *M. chelonae*, alters antibiotic resistance and expression of genes known to influence antibiotic resistance. How the presence of the prophage alters gene expression and antibiotic resistance is not understood.

It is possible that prophage gene products are driving changes in mycobacterial host gene expression. The most highly expressed gene in the BPs genome during lysogeny is the immunity repressor, gp33 (Figure 4) (Molloy, unpublished). The role of the immunity repressors, including gp33, is to bind operator sequences in the phage genome and regulate transcription (Villanueva, 2015). If gp33 also binds to sequences in the *M. chelonae* genome that are similar to the gp33 operator sequence, gp33 could be regulating transcription of *M. chelonae* genes. There are eight sequences in the *M. chelonae* genome that resemble the consensus operator sequence for gp33 (5′-CGACATATGTCG-3′), three of which are upstream of a *pad*R-like gene, the second most downregulated gene in the BPs-*M. chelonae* lysogen RNAseq data set (Hutchison, personal communication). It is unknown if gp33 is binding to these operator sites or is responsible for the changes in *whi*B7 and *pad*R expression and antibiotic resistance in the BPs-*M. chelonae* lysogen.

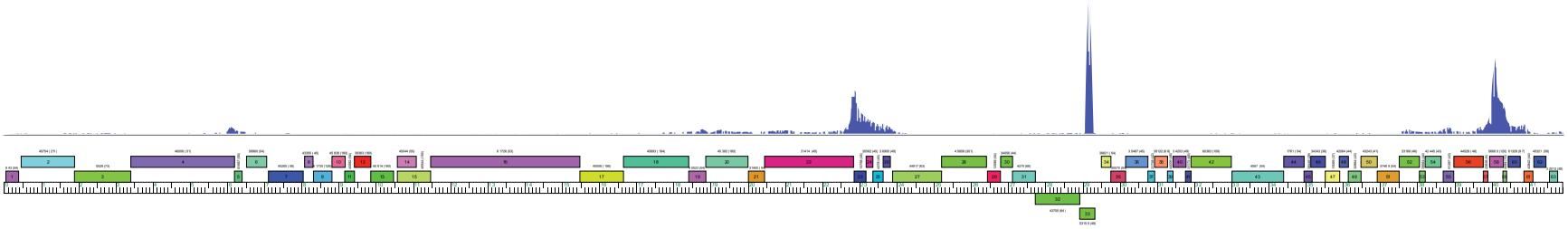

Figure 4. RNAseq reads mapped to the BPs genome. Reads indicate level of RNA expression. The immunity repressor, gp33, is the most highly expressed gene.

MATERIALS & METHODS

Bacterial Strains and Growth Conditions

Mycobacteria were grown in liquid 7H9 media supplemented with 10% oleic acid-albumin-dextrose (OAD) (Difco, Franklin Lakes, NJ), 1 mM $CaCl_2$, and 0.05% Tween 80 with shaking at 250 rpm or on Difco 7H10 agar supplemented with OAD. *M. chelonae* Bergey (ATCC: 19535; NZ_CP010946.1) and *M. smegmatis* mc^2155 (ATCC: 700084; NC_008596.1) cultures were grown at 30°C and 37°C, respectively. *Escherichia coli* 5-alpha (New England Biolabs (NEB), Ipswich, MA) cultures were grown in liquid Luria broth (Difco, Franklin Lakes, NJ) at 37°C with shaking at 250 rpm or on Luria agar supplemented with 50 μg mL^{-1} kanamycin (Difco).

Plasmid Construction

Plasmid pMH94 provided the backbone for pMHIR and pMHIattP and has previously been described (Lee et al., 1991). The plasmid pMH94 was digested with the restriction endonuclease *Sal*I, according to manufacturer's instructions (NEB, Ipswich, MA), to remove a 2,083-bp fragment containing the L5 integrase and L5 *att*P site (coordinates 906 – 2,989 of the pMH94 plasmid). Gel electrophoresis was performed to determine pMH94 had been successfully digested with *Sal*I via the presence of 2,083-bp and 4,136-bp fragments. The 4,136-bp fragment, lacking the L5 integration cassette, was captured via a Lonza FlashGel™ Recovery Cassette according to manufacturer's instructions (Lonza, Basel, Switzerland). Primers were designed using Primer3 (Untergasser et al., 2012) to amplify target regions of the BPs genome (Table 1). Plasmids pMHIR and pMHIattP were constructed as described by Sampson et al (2009). Fragment

BPsIR (BPs **I**ntegrase **R**epressor) includes the BPs integrase (gp32), immunity repressor (gp33), *att*P site within gp33, and intergenic region between gp33 and gp34 (Figure 3). Fragment BPsIattP includes the BPs integrase (gp32), the *att*P site within gp33, and 221-bp upstream of the *att*P site (Figure 3). The BPsIattP fragment does not include the entire repressor gene sequence (gp33) and therefore served as a control for the BPsIR sequence.

A second PCR reaction was performed using 60-mer primers that are specific to 30-bp of the flanking region of each insert and to 30-bp of the ends produced by *Sal*I digestion of the pMH94 plasmid. Gibson Assembly cloning reactions containing the *Sal*I-digested pMH94 plasmid and the control and experimental PCR products, BPsIattP and BPsIR, respectively, were performed in reaction ratios of insert to plasmid of 2:1 and 3:1 according to the manufacturer's recommendations (NEB) (Figure 5). Cloning products were transformed into competent *E. coli* cells (NEB) and plated onto Luria agar plates containing 50 μg mL^{-1} of kanamycin to select for cells with integrated plasmids. Plates were incubated at 37 °C overnight. Transformed colonies were grown overnight at 37 °C in 5 mL of Luria broth (Miller) containing 50 μg mL^{-1} of kanamycin. Plasmid DNA was isolated via the Wizard Plus SV MiniPrep DNA Purification System (Promega, Madison, WI) according to the manufacturer's instructions. DNA sequencing was performed to confirm cloning of correct sequences.

Table 1. PCR primer sequences.

Primer name	Primer sequence	Amplicon size	Coordinates
gp32attP+221_ forward	5′-CGCTGCCAGACCCCAATTGCGGAAC-3′	1,575	29,135 – 27,722
gp32attP+221_ reverse	5′-CTACTGATCGCGCGCCTTGAAGCTG-3′	1,827	
gp32attPgp33IG_reverse	5′-CGGTTGGGGTCATGTGCACCAACATAG-3′		906 –2,480
pMH9432attP+221_ reverse	5′-CCCGGCCAAGCTTGCATGCCTGCAGGTCGACTACTGATCGCGCGCCTT-3′	1,635	
pMH94gp32attPgp33IG_ forward	5′-CGAGCTCGGTACCCGGGGATCCTCTAGAGCGCTGCCAGACCCCAATTGCGGAAC-3′	1, 887	906 –2,731
pMH94gp32attPgp33IG_ reverse	5′-CGGCCAAGCTTGCATGCCTGCAGGTCGACGGTTGGGGTCATGTGCACCAACATAG-3′		
BPs_attP_left	5′-GCTTTATCCAGGGTTGACCA-3′	203	
BPs_attP_right	5′-GTTCCGATTATTGGCTGGA-3′	514	
BPs_attB_left	5′-GTCTCGTTACTGGCGAGCTT-3′	548	
BPs_attB_right	5′-CGGGTAGTAGGCAGATGAGC-3′	238	
BPs_attB_left			

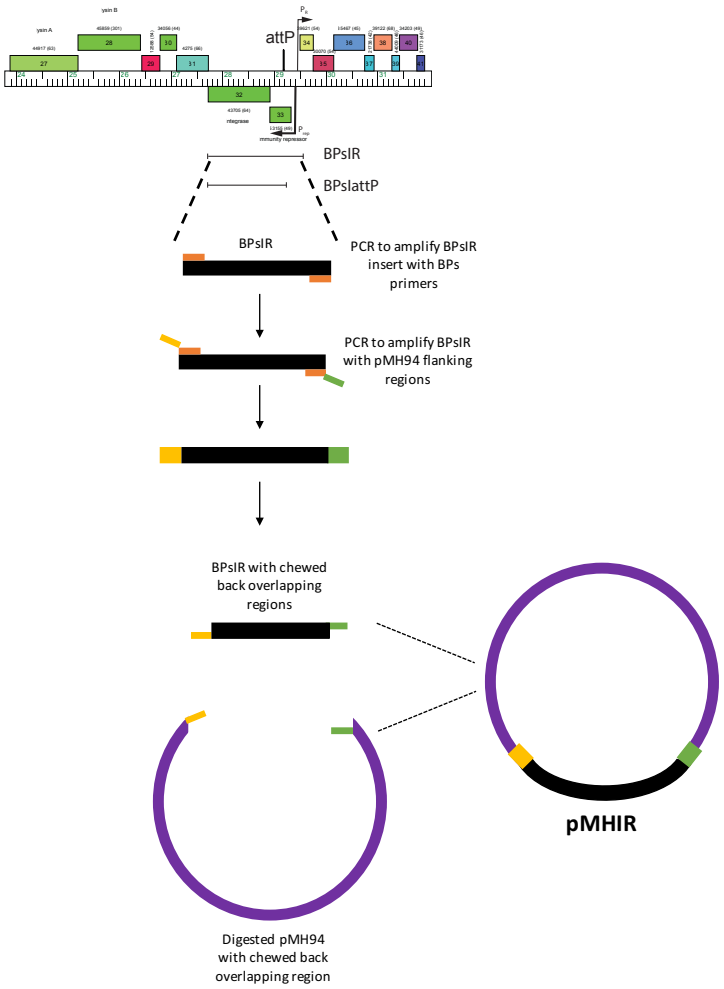

Figure 5. Gibson Assembly Cloning of insert BPsIR into *Sal*I-digested pMH94 plasmid vector, adapted from Gibson et al. (2009). Primers were designed to amplify a 1,826-bp fragment from the BPs genome (29,521 – 27,696) called BPsIR and a 1,575-bp control insert (29,270 – 27, 696) called BPsIattP. Fragments were amplified via PCR and inserted into a plasmid vector via Gibson Assembling Cloning to create pMHIR and pMHIattP, respectively.

Agarose Gel Electrophoresis

PCR products were separated on a 2% SeaKem® LE Agarose gel in 1X TAE buffer (40 mM Tris-acetate, 20 mM acetic acid, 2 mM Ethylenediaminetetraacetic acid). Gels were stained with SYBR™ Safe DNA Gel Stain and visualized on the Azure Biosystems C200 Imaging System.

Electroporation of *M. chelonae* Cells

Electrocompetent *M. chelonae* cells were prepared by washing log-phase *M. chelonae* cells in ice-cold 10% glycerol according to De Moura et al (2012). Plasmid DNA in concentrations of 100, 300, and 500 ng was electroporated into 100 µL of electrocompetent *M. chelonae* with a single pulse (2.5 kV, 25 mF, and 1,000 Ω). Cells were allowed to recover in 900 µL of 7H9-OAD at 30 °C for 4 h before plating onto 7H10 agar containing 250 µg mL^{-1} of kanamycin. Plates were incubated at 30 ℃ for 5–6 d. Primer pairs were designed to detect the BPs *att*L and *att*R sites, and the L5 *att*L and *att*R sites to verify integration of pMHIattP and pMHIR plasmids and the control plasmid (undigested pMH94), respectively, into the *M. chelonae* genome (Figure 6). Transformants were picked and PCR screened for the presence of *att*L and *att*R sequences.

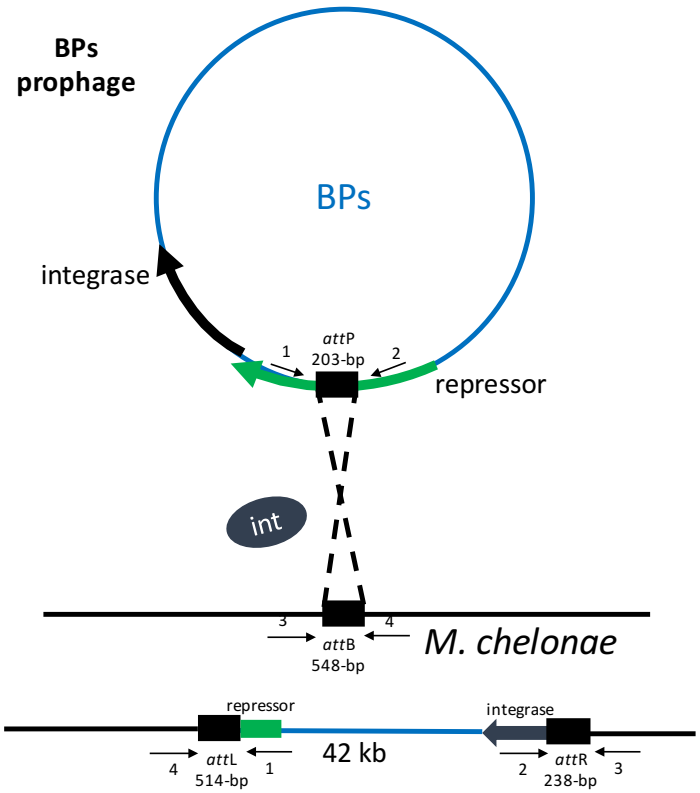

Figure 6. Model of BPs genome integration into the bacterial genome. Integration is catalyzed by the phage integrase acting on identical sequences, *att*P and *att*B, on the phage and bacterial genomes, respectively. Upon integration, the *att*L and *att*R sites are present in the lysogen. Integration of the plasmids pMHIR and pMHIattP occurs in the same manner. To detect integration of the BPs genome or plasmids pMHIR and pMHIattP, primers were designed to bind to sequences flanking the BPs *att*P (primers 1 and 2) and *att*B sites (primers 3 and 4. Upon integration, primers 1 and 4 will amplify the *att*L site, while primers 2 and 3 will amplify the *att*R site.

Immunity Assays

Cultures were grown to an optical density (OD_{600}) of ≥ 5 and plated in 4.5 ml of 7H9 top agar onto L agar plates. Serial 10–fold dilutions of BPs lysate were applied in 5-µL quantities onto lawns of *M. chelonae* WT, *M. chelonae* (pMHIR) and *M. chelonae* (pMHIattP). Plates were incubated at 30 °C for 48 h and screened for plaques.

RNA Isolations and qRT-PCR Assays

Cultures of *M. chelonae* were grown to an OD_{600} of 0.8 or 1.0. Cells were harvested in a quantity of 4 mL, in replicates of 8, into 8 ml of RNAprotect Bacteria reagent (Qiagen, Hilden, Germany) and incubated for 5 min at RT. Cells were centrifuged at 5,000 x *g* for 10 min. Supernatant was removed and the cell pellets were resuspended in 100 µL of TE containing 20 mg mL of lysozyme (Sigma Aldrich, St. Louis, MO). After incubating for 40 min at RT, 700 µL of RLT buffer containing β-mercaptoethanol was added to cell suspensions (Qiagen). Cells were lysed in 2-mL Lysing Matrix B tubes (MP Biomedicals) and homogenized for 8 min at 50 Hz in the Qiagen TissueLyser LT using an ice-cold tube adapter. Total RNA was isolated from lysates using the RNeasy Mini Kit (Qiagen) according to the manufacturer's recommendations. To remove genomic DNA, samples were treated with DNAseI (Qiagen) on the column according to the manufacturer's recommendations. To ensure that all genomic DNA was removed from RNA samples, a second DNase treatment (Turbo DNase, Life Technologies) was conducted after elution from RNeasy Mini Kit columns. The quantity and quality of RNA was determined via analysis with Nanodrop One spectrophotometer (Thermo Fisher Scientific) and FlashGel™ RNA system (Lonza).

cDNA was synthesized from 500 ng of RNA in 20-µL reaction volumes using the Quantabio qScript Synthesis kit, according to the manufacturer's instructions (Quantabio, Beverly, MA). Samples were diluted 1:6 in 10 mM Tris-HCl and cDNA was used to conduct quantitative real-time PCR assays to analyze gene expression levels. Template cDNA was added in volumes of 1 µL (0.02 ng μL^{-1}) to triplicate 25-µL qRT-PCR reactions containing 1x Perfecta qPCR Supermix (Quantabio), 200nM of each gene-specific primer. Reactions were run under the following program in the Bio-Rad CFX96 Real-Time system (Bio-Rad Laboratories, Hercules, CA): 95 °C for 3 min followed by 40 cycles of 95 °C for 10 s, 60 °C for 30 s and 65 °C for 5 s, and 65 °C for 5 s. Gene expression was measured with SYBR Green and reported expression levels are indicative of $2^{-\Delta\Delta Ct}$ (Livak, KJ., 2001). Significant differences in expression were determined by ANOVAs conducted with JMP statistical discovery software and significance was indicated by $P < 0.05$ (Jones, B., Sall, J., 2011).

MIC Assays

To analyze the impact of gp33 on *M. chelonae* antibiotic resistance, minimum inhibitory concentration (MIC) assays were conducted. *M. chelonae* WT, BPs lysogen, and recombinant strain cultures were grown overnight to an OD_{600} of 0.1–0.3 in 7H9-OAD + 0.05% Tween 80 media (Middlebrook). Cultures were diluted to an OD_{600} of 0.005 and incubated at 30 °C with shaking for 4 h before applying cells in 50-µL quantities to 96 well plates containing 50 µL of 7H9 media with varying concentrations of antibiotics. Tetracycline and clarithromycin assays were performed using two-fold serial dilutions of the antibiotics (0.5 – 64 and 0.19 – 25 µg mL^{-1}, respectively). Clarithromycin was prepared in DMSO, therefore an equivalent amount of DMSO was included in all wells. Each strain

was tested at each antibiotic concentration in replicates of six and no-antibiotic controls and no bacteria controls were performed in replicates of 16. Inoculated plates were sealed with sterile porous seals (VWR), wrapped in Parafilm (Bemis, Neenah, WI) and incubated at 30 °C for 2 d before adding 1 µL of AlamarBlue (BioRad, Hercules, CA). After incubation at 30 °C for 1 d, the optical density (OD) was measured at 570- and 600 nm and the percent viability of cells was calculated as the percent difference between antibiotic-treated cells and untreated cells according to the manufacturer's instructions. Each assay was replicated in three independent experiments.

RESULTS

Gene Expression Profile of the BPs Prophage in *M. chelonae* WT

To determine which genes are expressed from the BPs prophage genome during lysogenic infection of *M. chelonae,* RNA was isolated from BPs-*M. chelonae* lysogens and submitted for RNAseq analysis. RNAseq reads were aligned to the BPs genome (Figure 4). The two most highly expressed genes of the BPs genome were the immunity repressor, gp33, and a gene of unknown function within the mycobacterial phage mobile element (MPME), gp58. There were also low levels of reads mapped to BPs gp5 and gp23–36.

Construction of BPs gp33 Expression Plasmids, pMHIR and pMHIattP

The recombinant strain *M. chelonae* (pMHIR) that expresses the BPs immunity repressor and the control strain *M. chelonae* (pMHIattP) were created to test the effect of the BPs repressor on bacterial gene expression and antibiotic resistance. Plasmids pMHIR and pMHIattP were constructed using plasmid pMH94 and the amplified fragments (Figure 5 and Figure 7) (Lee et al., 1991). This plasmid contains a kanamycin resistance gene but lacks a mycobacterial origin of replication and therefore cannot be maintained in a bacterial cell unless it has integrated into the bacterial genome via a plasmid-encoded integrase cassette. The 2,083-bp L5 integrase cassette was removed by digesting pMH94 with *Sal*I endonuclease and replaced with the BPs integration cassette. Two variations of BPs integration cassette inserts were PCR amplified from the BPs genome. The first insert, BPsIR, includes sequences for the BPs integrase (gp32), *att*P site, immunity repressor (gp33), and P_{rep} (promoter for gp33) (Figure 3). The control insert, BPsIattP, encodes the integrase, *att*P site, and 221-bp upstream of the *att*P site (Figure 3). The PCR products were

cloned into *Sal*I-digested pMH94 using Gibson cloning resulting in plasmids pMHIR and pMHIattP (Figure 7). Plasmid insert sequences were confirmed by sequencing.

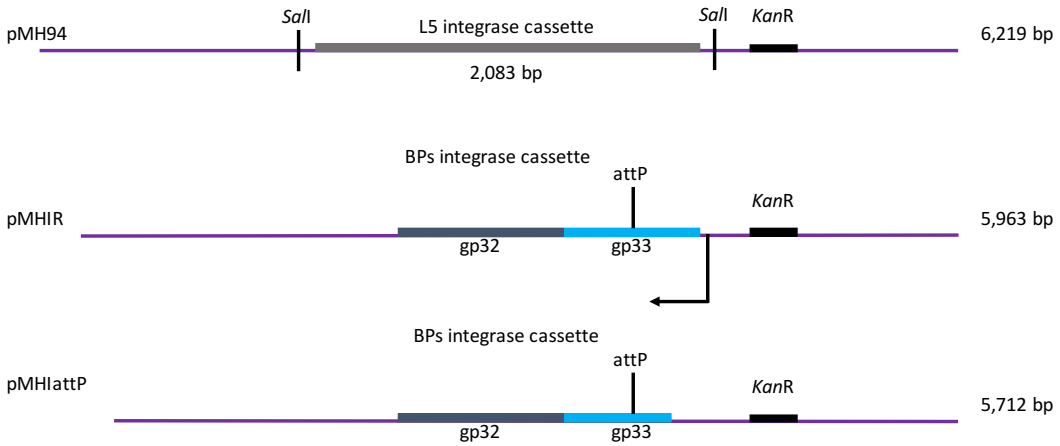

Figure 7. Experimental design of integrative plasmids pMHIR and pMHIattP encoding BPs integrase cassette as described by Sampson et al. pMHIR encodes the integrase gene (gp32), the phage attachment site *att*P, the immunity repressor (gp33), and the intergenic region between gp33 and gp34 that includes the gp33 promoter (indicated by black arrow). pMHIattP encodes the integrase gene (gp32), the *att*P site, and an additional 221-bp upstream of the attP site. pMHIattP is missing the promoter and 5′end of the gp33 gene.

After electroporation of plasmids into *M. chelonae,* recombinant strains were validated via PCR and agarose gel electrophoresis using primers specific to BPs sequences flanking the phage attachment site, *att*P (primers 1 and 2) and sequences flanking the bacterial attachment site, *att*B (primers 3 and 4). Upon successful integration, primers 1 and 4 produced a 514-bp product and 2 and 3 produced a 238-bp product, which were consistent with the size of PCR amplification from the integration attachment sites *att*L and *att*R, respectively (Figure 8).

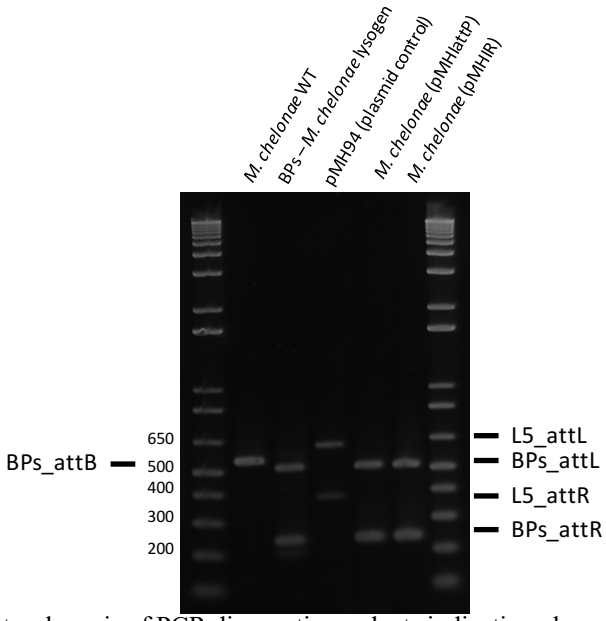

Figure 8. Agarose gel electrophoresis of PCR diagnostic products indicating phage attachment sites, attL and *att*R, detected in recombinant and lysogen strains of *M. chelonae.* Attachment sites, *att*L and *att*R, were detected in DNA isolated from BPs-*M. chelonae* lysogen (lane 3), and recombinant *M. chelonae* carrying plasmids pMHIR (lane 6) and pMHIattP (lane 5). As a control, PCR was also performed on *M. chelonae* WT DNA (lane 2) to amplify the bacterial *att*B site and *M. chelonae* (pMH94) (lane 4) was used as an integration control for the recombinant strains. *M. chelonae* (pMH94) carries the L5 integration cassette with the L5 *att*L and L5 *att*R. Lanes 1 and 7 contain the molecular size markers. Expected product sizes: BPs *att*B – 548 bp (Lane 2), BPs*att*L – 514 bp (Lane 3, 5, 6), BP*satt*R – 238 bp (Lane 3, 5, 6), L5*att*L – 623 bp (Lane 4), L5*att*R – 385 bp (Lane 4).

To determine if a functional gp33 immunity repressor is produced from the integrated plasmid pMHIR, superinfection immunity assays were performed on *M. chelonae* (pMHIR) and control strain *M. chelonae* (pMHIattP) (Figure 9). *M. chelonae* (pMHIR) was immune to infection by BPs, indicating expression of a functional repressor, whereas, *M. chelonae* (pMHIattP) was susceptible to infection by BPs.

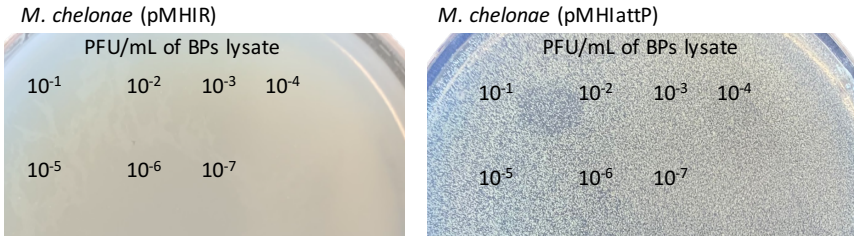

Figure 9. To determine if the recombinant plasmid pMHIR produces functional immunity repressor in *M. chelonae*, a superinfection immunity assay was performed. Serially diluted BPs lysate was applied to lawns of *M. chelonae* (pMHIR) and *M. chelonae* (pMHIattP).

Gp33 Transcription Levels are Comparable Between Recombinant Strains and BPs-*M. chelonae* Lysogens

To confirm expression of gp33 from recombinant strains, qRT-PCR was performed on RNA isolated from *M. chelonae* (pMHIR) and *M. chelonae* (pMHIattP). In cells grown to optical densities of 0.8, gp33 expression was 4-fold lower in the recombinant strain *M. chelonae* (pMHIR) than the BPs-*M. chelonae* lysogen strain (Figure 10A). Expression of gp33 was comparable to that of the BPs-*M. chelonae* lysogens in cells grown to optical densities of 1.0 (Figure 10B).

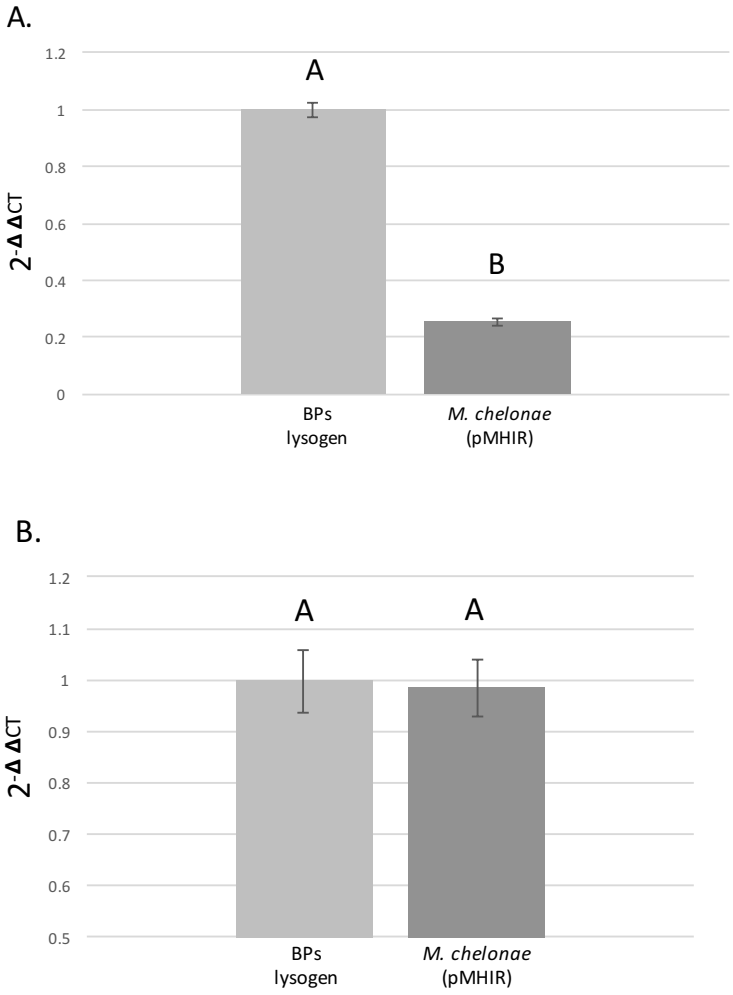

Figure 10. The average relative expression of BPs gp33 in BPs-*M. chelonae* and *M. chelonae* (pMHIR) cells grown to an optical density of 0.8 (A) (F = 62.96, P = 0.0014) and 1.0 (B) (F = 0.0015, P = 0.9705, not significant) as measured with SYBR Green quantitative RT-PCR. Graphs are indicative of averages +/- the standard errors of the mean, n = 3. Letters indicate which strains are statistically different.

Gp33 has Minimal Impact on the Expression of *M. chelonae* Genes *whi*B7 and *pad*R

To determine if gp33 is responsible for the induction of *whi*B7, qRT-PCR assays were performed on RNA isolated from *M. chelonae* WT, BPs-lysogens and the recombinant strains. *whi*B7 expression was 50-fold greater in the BPs-*M. chelonae* lysogen relative to *M. chelonae* WT strain. *whi*B7 was not elevated in the recombinant strain relative to the *M. chelonae* WT control strain. At cell densities of 0.8, *whi*B7 expression in *M. chelonae* carrying pMHIattP and pMHIR was nearly equivalent to that of *M. chelonae* WT with fold changes of 1.5 and 1.1, respectively (Figure 11A). At cell densities of 1.0, expression of *whi*B7 was increased in the recombinant strains but was not significantly upregulated in the *M. chelonae* (pMHIR) strain compared to the *M. chelonae* (pMHIattP) strain with fold changes of 3.5 and 2, respectively (Figure 11B).

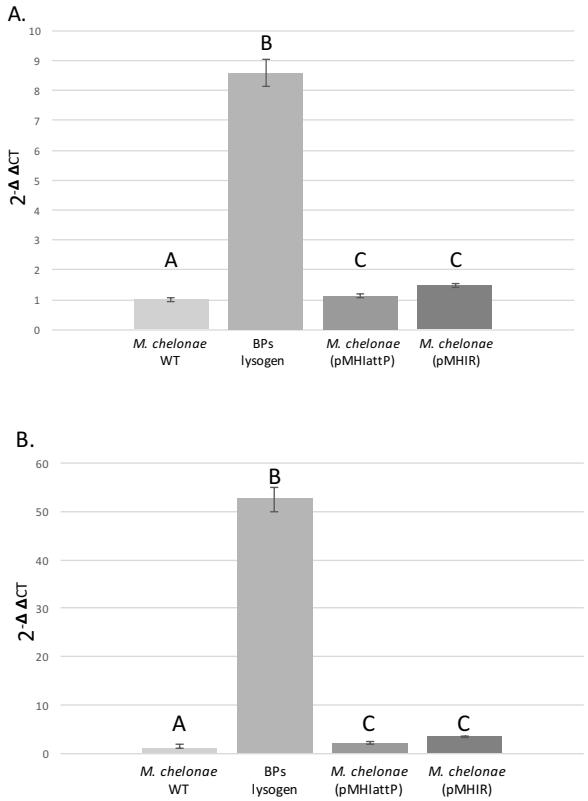

Figure 11. Average relative expression of *M. chelonae* *whi*B7 in cells grown to an optical density of 0.8 (A) (F = 3176.83, P < .0001) and 1.0 (B) (F = 164.87, P < .0001) as measured with SYBR Green quantitative RT-PCR. Graphs are indicative of averages +/- the standard errors of the mean, n = 3. Letters indicate which strains are statistically different.

Due to possible vector-specific effects, it is difficult to determine the impact of gp33 on *pad*R expression. There was no significant difference in *pad*R expression in the pMHIR strain relative to the plasmid control strain at cell densities of 0.8. *pad*R expression was decreased by 2-fold in both recombinant strains compared to *M. chelonae* WT and the difference between the two plasmid strains was not significant (Figure 12A). In cells grown to a higher density of 1.0, the vector appeared to have an inducing effect as both recombinant strains express *pad*R at levels 5–6-fold higher than *M. chelonae* WT, and there was no significant difference between the recombinant strains (Figure 12B).

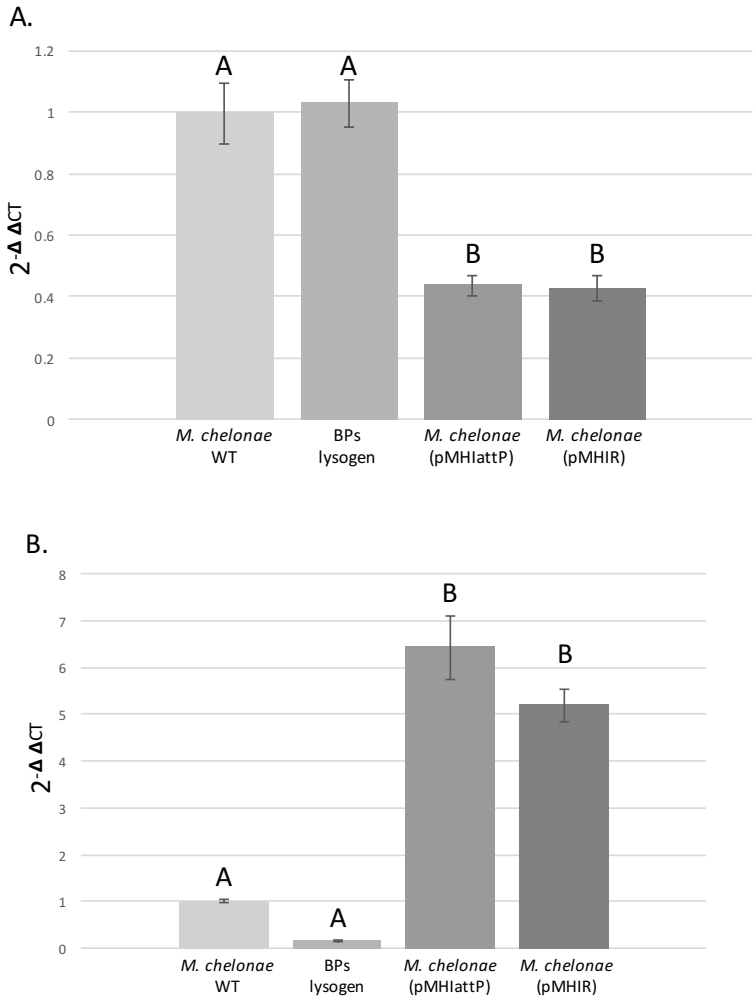

Figure 12. Average relative expression of *M. chelonae pad*R in cells grown to an optical density of 0.8 (A) (F = 893.97, P < .0001) and 1.0 (B) (F = 28.4137, P < .0001) as measured with SYBR Green quantitative RT-PCR. Graphs are indicative of averages +/- the standard errors of the mean, n = 3. Letters indicate which strains are statistically different.

The Effect of gp33 Expression on *M. chelonae* Antibiotic Resistance

To measure the effect of gp33 expression on the antibiotic resistance of *M. chelonae*, MIC assays were performed on recombinant strains and compared to *M. chelonae* WT and BPs-*M. chelonae* lysogen strains. Expression of gp33 did not appear to alter antibiotic resistance. There was no significant difference in resistance to tetracycline between the two recombinant strains relative to *M. chelonae* WT (Figure 13A). *M. chelonae* (pMHIattP) treated with acivicin, an inducer of *whiB7* expression, did not show overall increased resistance to tetracycline compared to *M. chelonae* (pMHIR) and *M. chelonae* (pMHIattP). These results are not comparable to the BPs-*M. chelonae* lysogen, which shows increased resistance at increasing concentrations of tetracycline. In the presence of clarithromycin, *M. chelonae* (pMHIR) did show increased resistance at concentrations of 0.20-25 μg mL^{-1} compared to *M. chelonae* (pMHIattP) and *M. chelonae* (pMHIattP) plus acivicin (Figure 13B). However, a dose-dependent response was not seen and therefore this assay needs to be repeated before a conclusion about the impact of gp33 on resistance to clarithromycin can be made.

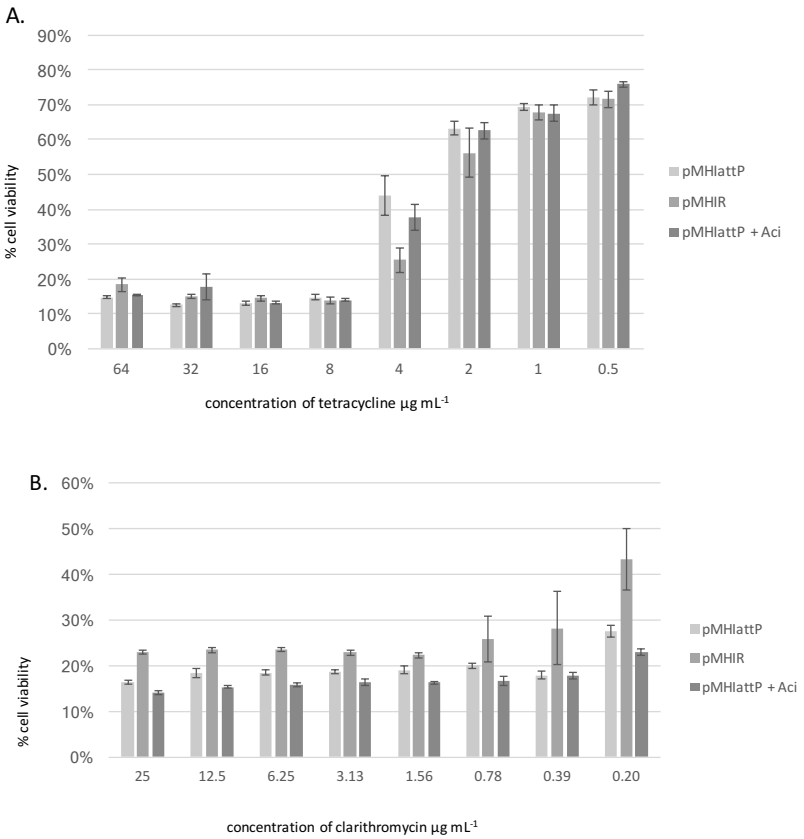

Figure 13. Percent viability of cultures after treatment with clarithromycin (A) and tetracycline (B). Graphs represent average values +/- SE of the mean, $n = 6$. The optical density of cultures was measured at 570 and 600 nm. Bars indicate the percent difference in cell viability between antibiotic-treated and untreated cells.

The Effects of Co-Expression of BPs gp5 and the Immunity Repressor gp33 on *M. chelonae* Gene Expression

Because gp33 expression was lower than that of the BPs-*M. chelonae* lysogen when grown to densities of 0.8, and because gp33 expression alone did not appear to impact *whi*B7 nor *pad*R expression, we were curious if the co-expression of gp5 and gp33 would increase expression of gp33 and possibly drive changes in *pad*R. A plasmid encoding BPs gp5 was constructed from plasmid pMO01 (Dedrick et al., 2016), which has a constitutive *M. bovis* Heat Shock Protein (hsp) promoter and is maintained by a *parABS* partitioning system from mycobacteriophage RedRock (Dedrick et al., 2016). If gp5 affects expression of gp33, we expect to see higher gp33 expression levels from *M. chelonae* (pMHIR) in the

presence of gp5 relative to *M. chelonae* (pMHIR) strains with the empty pMO01 vector. To verify the presence of the plasmids, recombinant strains were analyzed by PCR during the culture process prior to RNA isolations. The plasmids were lost during subculturing just prior to RNA isolations, yet we still saw differential gene expression (PCR data not shown). Levels of gp33 transcript were nearly 2-fold higher in *M. chelonae* carrying pMHIR and gp5 relative to strains carrying pMHIR and empty pMO01 vector, although the difference was not statistically significant (Figure 14). *pad*R expression was not significantly down-regulated in the *M. chelonae* recombinant strain carrying pMHIR and gp5 when compared to *M. chelonae* carrying pMHIR and empty vector pMO01 (Figure 15). *pad*R expression levels in *M. chelonae* carrying pMHIR and empty vector and *M. chelonae* carrying pMHIR and gp5 were decreased by 0.7- and 0.8-fold, respectively, indicating that the presence of the pMO01 plasmid may have a slight suppressive effect.

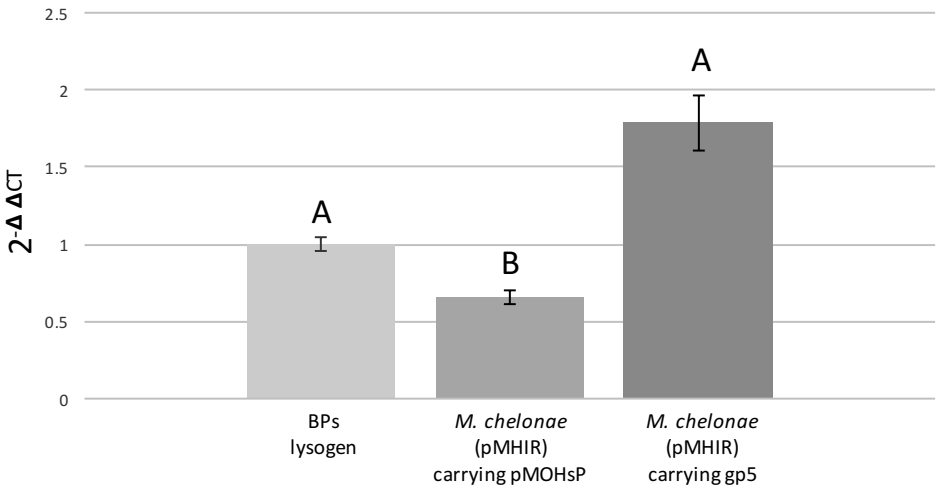

Figure 14. Average relative expression of BPs gp33 in cells grown to an optical density of 1.0 as measured with SYBR Green quantitative RT-PCR ($F = 18.07$, $P = 0.0029$). Graphs are indicative of averages +/- the standard errors of the mean, $n = 3$. Letters indicate which strains are statistically different.

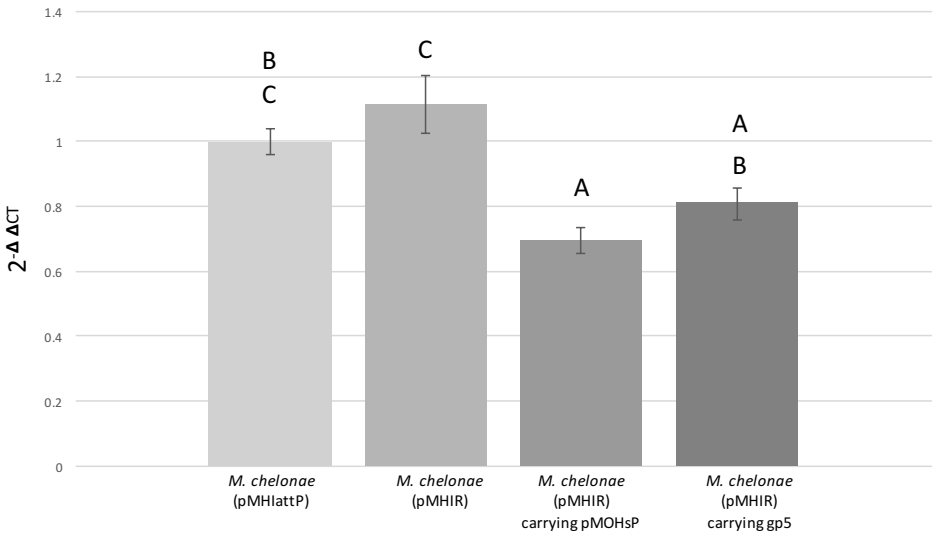

Figure 15. Average relative expression of BPs *pad*R in cells grown to an optical density of 1.0 as measured with SYBR Green quantitative RT-PCR. Graphs are indicative of averages +/- the standard errors of the mean, $n = 3$ ($F = 10.49$, $P = 0.0038$). Letters indicate which strains are statistically different.

DISCUSSION

Mycobacteria, including *M. abscessus* and *M. tuberculosis* are becoming increasingly drug resistant and there is a need for alternative therapeutics (Lee et al., 2015). One mechanism of mycobacterial pathogenicity and antibiotic resistance that is not well understood is the role of prophage. Prophage (viruses that integrate their genomes into that of the host) likely increase the pathogenicity of mycobacterial hosts, but it is unknown *how* (Fan et al., 2016). Upon lysogenic infection, the prophage BPs causes significant differential expression of 7.74% of genes in the *M. chelonae* genome, including *whi*B7, a known regulator of antibiotic resistance genes, and *pad*R, a gene associated with antibiotic resistance in other bacterial species (Burian et al., 2012, Park et al., 2017). The most highly upregulated BPs gene during lysogenic infection is the viral immunity repressor, gp33. Our hypothesis was that if the BPs immunity repressor (gp33) is responsible for the changes we see in the BPs-*M. chelonae* lysogen compared to *M. chelonae* WT, then a recombinant strain of *M. chelonae* expressing gp33 at levels comparable to that in the BPs lysogen should show similar gene expression and antibiotic resistance changes as the BPs-*M. chelonae* lysogen.

The immunity repressor, gp33, is the most highly expressed gene in the BPs genome during lysogenic infection of *M. chelonae* and is the most logical candidate for altering mycobacterial gene expression (Figure 4). Phage immunity repressors are typically highly expressed during lysogeny (Dedrick et al., 2013., Dedrick et al., 2019). This is expected because high quantities of the immunity repressor are needed to repress lytic gene expression and maintain lysogeny (Petrova, 2015). Gp58 is also highly expressed, but

based on unpublished data from the Molloy lab, it likely does not play a role in *whi*B7 expression. Gp58 is a novel *Mycobacterium* phage mobile element (MPME) found in some Cluster G phage (Sampson et al., 2009). There is no known function for gp58, but because it is the only ORF in the mobile element, it could be a recombinase and have DNA binding abilities. The Molloy lab has investigated *whi*B7 expression in *M. chelonae* carrying a prophage identical to BPs but lacks gp58 and *whi*B7 expression is elevated, suggesting gp58 is not playing a role in *whi*B7 expression (Molloy, personal communication). There are other genes expressed during BPS lysogeny at very low levels, including gp23-26, which are thought to be due to background lytic infection given their location within an operon of structural genes. There is always some background lytic gene expression within a lysogenic population (Nanda et al., 2015). We assumed the same for gp5, but given its predicted function as a ribosomal modulation factor, which can help stabilize 70S ribosomes to facilitate leaderless transcription, we sought to determine if co-expression of gp5 and gp33 increased gp33 levels, as gp33 is expressed as a leaderless transcript (Broussard et al., 2013). Overall, we chose to investigate further the immunity repressor, BPs gp33, given it is the most highly expressed gene and functions as a transcriptional regulator to alter gene expression.

Gp33's function as an immunity repressor and transcriptional regulator strengthens its candidacy for a regulator of bacterial gene expression. In the BPs phage, the gp33 tetramer binds to palindromic operator sequences upstream and overlapping BPs lytic gene promoters with the conserved sequence 5′-CGACATATGTCG-3′ (Villanueva, 2015). Binding to these operator sites represses the transcription of these genes (Villanueva, 2015). If there are sequences within the *M. chelonae* genome that overlap regulatory

sequences, it is possible that gp33 could be binding to and regulating transcription of bacterial genes. Eight such sequences were found in gene regulatory regions in the *M. chelonae* genome, three of which are located upstream of the second most downregulated gene in the BPs-*M. chelonae* RNAseq set, *pad*R (Hutchison, personal communication). PadR-like transcription factors contain a winged helix-turn-helix domain in the N-terminal that interacts with palindromic operator DNA sequences (Park et al., 2017). The function of this PadR-like transcriptional regulator in *M. chelonae* is not known; however, in other bacterial species *pad*R genes regulate genes involved in environmental stress responses (Park et al., 2017). This includes responses to phenolic acid, antibiotics, and other toxic compounds detected in the environment (Park et al., 2017). We do not know if *pad*R in *M. chelonae* regulates antibiotic resistance genes, but given the increased antibiotic resistance of BPs-*M. chelonae* lysogens, it could be contributing to resistance. To show that *pad*R is contributing to resistance, MIC assays would need to be run on an *M. chelonae pad*R deletion strain and *M. chelonae pad*R overexpression strain. To determine if gp33 drives changes in *whi*B7 and *pad*R expression and antibiotic resistance in *M. chelonae*, a recombinant strain of *M. chelonae* that expresses gp33 in its active form was created.

A recombinant strain of *M. chelonae* (pMHIR) that expresses a functional immunity repressor was successfully created according to Sampson et al (2009). *M. chelonae* (pMHIR) carries pMHIR that has integrated into the BPs *att*B site and encodes the BPs integrase and immunity repressor (Figure 7). A plasmid control strain, *M. chelonae* (pMHIattP) was successfully created that encodes the integrase (gp32) and *att*P site but lacks an intact gp33 gene. The *M. chelonae* (pMHIR) strain demonstrates superinfection immunity, which indicates that gp33 expressed from pMHIR is functional and capable of

binding operator sequences and inhibiting transcription (Figure 9). qRT-PCR analyses indicate that the level of transcript expressed from pMHIR is comparable to that of BPs-*M. chelonae* lysogens when RNA is harvested from cells at a density of 1.0 (Figure 10B). Given that a functional immunity repressor is present and transcript levels are comparable to that of the BPs-*M. chelonae* lysogen, changes in *whi*B7 and *pad*R should be detected in *M. chelonae* (pMHIR) if gp33 is responsible for the gene expression changes in the lysogen.

The BPs immunity repressor (gp33) does not appear to be responsible for *whi*B7 induction. Based on qRT-PCR analyses, w*hi*B7 expression is 8-fold to 50-fold higher in the BPs-*M. chelonae* lysogen than in *M. chelonae* WT in cells grown to an optical density of 0.8 and 1.0, respectively (Figure 11A and 11B). If gp33 were responsible for the changes we see in *whi*B7 expression, we would expect to see similar expression levels in *M. chelonae* (pMHIR) compared to the BPs-*M. chelonae* lysogen. *whi*B7 was not expressed in *M. chelonae* (pMHIR) at levels comparable to that of the BPs-*M. chelonae* lysogen at an optical density of 0.8 nor 1.0. *whi*B7 expression was not significantly higher in the recombinant strain *M. chelonae* (pMHIR) compared to the plasmid control strain *M. chelonae* (pMHIattP). Therefore, BPs gp33 is not likely responsible for the increase in *whi*B7 expression upon lysogenic infection of *M. chelonae*.

Gp33 also does not appear to be involved in *pad*R downregulation. *pad*R was the second most downregulated gene in *M. chelonae* according to RNAseq analysis. When qRT-PCR analyses were run on cells grown to an optical density of 0.8, *pad*R was not significantly downregulated in the BPs-*M. chelonae* lysogen strain compared to the *M. chelonae* WT strain (Figure 12A). When cells are grown to an optical density of 1.0, the

same density used for RNAseq studies, *pad*R expression decreases drastically and transcripts are hardly detectable in the BPs-*M. chelonae* lysogen compared to the *M. chelonae* WT strain, thus supporting RNAseq data (Figure 12B). At an OD_{600} of 1.0, expression of gp33 leads to slightly downregulated *pad*R levels relative to the control recombinant strain, but the difference is not significant (Figure 12B). Interestingly, *pad*R expression is lower in both recombinant strains at an OD_{600} of 0.8 relative to the *M. chelonae* WT strain, suggesting that at densities of 0.8 the vector has a suppressive effect. But *pad*R expression is higher in both recombinant strains relative to *M. chelonae* WT at an OD_{600} of 1.0, suggesting the vector induces *pad*R at densities of 1.0. If gp33 is responsible for the *pad*R repression observed in the BPs-*M. chelonae* lysogen grown to a density of 1.0, we expect to see negligible levels of *pad*R expression in the recombinant strain *M. chelonae* (pMHIR) grown to a density of 1.0. These data suggest that gp33 does not appear to be responsible for *pad*R downregulation in the lysogen and downregulation of *pad*R in the lysogen strain is density-dependent.

While we do not know why there is a difference in *pad*R expression at different densities, bacterial population density has been connected to gene expression regulation (Bassler, B., 1999, Bharati, B., Chatterji, D., 2013, Zhao et al., 2020). This is perhaps because as the cells enters late-log and stationary phase, resources for transcription are altered (e.g. sigma and anti-sigma factors) (Klumpp, S., Hwa, T., 2014, Flentie et al., 2016). The effects of the prophage or plasmids on *pad*R expression would therefore be different depending on the transcription factors present in the cell at different densities (Park et al., 2017). As an alternative explanation, many bacteria, including mycobacteria, can participate in quorum sensing. Quorum sensing occurs as changes in population density

triggers the release of molecules, which signal the release of secondary messengers. These messengers carry the signal to effector molecules that alter cellular functions, including expression of genes involved in antibiotic resistance (Bharati, B., Chatterji, D., 2013, Zhao et al., 2020). As the population of *M. chelonae* cells increases, signals could trigger downregulation of *pad*R expression. Overall, given that the vector interfered with *pad*R expression, further studies are required to fully rule out gp33 as an inhibitor of *pad*R expression.

Gp33 does not appear to increase *M. chelonae* antibiotic resistance. This is unsurprising given that gp33 does not seem to alter transcription of genes involved in antibiotic resistance. MIC assays were performed with decreasing concentrations of tetracycline and clarithromycin, a drug typically used to treat *M. abscessus* infections. While *M. chelonae* (pMHIR) appears to show increased resistance to clarithromycin compared to *M. chelonae* (pMHIattP) and *M. chelonae* (pMHIattP) plus acivicin (a natural inducer of *whi*B7), a dose-dependent response is not seen (Figure 13B). We would expect to see little cell viability at a concentration of 25 μg mL^{-1} of clarithromycin and a steady increase in cell viability as the concentration decreases. Therefore, a conclusion from this data cannot be made. A dose-dependent response was seen in cultures grown in the presence of tetracycline. *M. chelonae* (pMHIR) did not show increased resistance to tetracycline compared to *M. chelonae* (pMHIattP) and *M. chelonae* (pMHIattP) plus acivicin (Figure 13A). Given that gp33 does not appear to be responsible for the induction of *whi*B7 in the BPs-*M. chelonae* lysogen, these findings are not surprising. It can be concluded that gp33 is not responsible for the increased antibiotic resistance of *M. chelonae* in the presence of the BPs prophage.

Although gp5 appears to be a lytic gene, we wondered if co-expression of gp5 and gp33 would impact gp33 expression levels. We were intrigued by BPs gp5 because of its predicted function as a ribosome modulation factor. Ribosome modulation factors stabilize 70s ribosomes to more efficiently initiate translation of leaderless transcripts, like the gp33 transcript (Broussard et al., 2013, Beck, H., Moll, I., 2018). Leaderless transcripts lack ribosome binding signals and binding of the 70s ribosome to the 5′ terminus stabilizes the mRNA and protects the transcript from degradation (Beck, H., Moll, I., 2018). Therefore, gp5 could potentially stabilize the gp33 transcript. The episomal plasmid expressing gp5 is maintained by a *par*ABS system (Dedrick et al., 2016). In the presence of pMHIR, the gp5 plasmid is unstable, indicating that the two plasmids are incompatible. Both plasmids were detectable at the beginning of culture growth, but the gp5 plasmid was lost just prior to RNA isolations. We were still able to observe an increase in gp33 expression in *M. chelonae* (pMHIR) strains carrying the gp5 plasmid (Figure 14). This effect was not observed in *M. chelonae* (pMHIR) strains carrying the empty plasmid vector for gp5. It is possible that gp5 protein produced prior to loss of the plasmid remained in cells after loss of the plasmid and had an effect on gp33 expression. Co-expression of gp5 and gp33 in *M. chelonae* does not lead to decreased *pad*R expression levels (Figure 15), again suggesting that gp33 most likely does not play a role in *pad*R regulation.

CONCLUSIONS & FUTURE WORK

This thesis project has contributed to the overall understanding of the role of prophage in the gene expression and antibiotic resistance of their bacterial hosts. My work has helped the Molloy lab determine that gp33 expression is likely not responsible for changes in *whi*B7 expression. Since the completion of this work, the Molloy lab has determined that a naturally occurring prophage must be present with the BPs prophage to change expression of *whi*B7. My work has helped to show that BPs lysogenic gene expression is not important for this interaction. Given that all cultures of bacterial lysogens contain a subset of cells undergoing induction (lytic phage infection), we are currently looking at the role of BPs lytic gene expression in the presence of the naturally occurring prophage as means of altering bacterial gene expression.

Future work will also investigate the roles of other prophage-encoded genes to determine if the expression of other virally-encoded genes is necessary to impact *M. chelonae* gene expression and antibiotic resistance. More work needs to be done to determine the impact of gp33 expression on *pad*R. Our lab is currently using a GFP reporter plasmid under the control of the *pad*R promoter to determine the impact of gp33 on expression. The strains I produced in this work will be used to test GFP expression in the presence or absence of gp33. Recombinant strains of *M. chelonae* lacking *pad*R or *whi*B7 or overexpressing *pad*R or *whi*B7 could be created to determine their respective effects on antibiotic resistance. Further analyses can be performed on the *M. chelonae* recombinant strain, *M. chelonae* (pMHIR), expressing gp5 to determine if co-expression of BPs genes gp33 and gp5 is needed to cause differential expression of *M. chelonae whi*B7 and

increased antibiotic resistance. The mobile genetic element of BPs, gp58, can also be transformed into *M. chelonae* to investigate its impact on *M. chelonae* gene expression. Overall, the outcome of this thesis was crucial to helping rule out lysogenic gene expression from prophage BPs as a driver of *whi*B7 expression in *M. chelonae*.

In conclusion, understanding the interaction between phage and their bacterial hosts is crucial to understanding antibiotic resistance mechanisms and treating antibiotic resistant infections. The work of my thesis has directly helped us understand more about how phage contribute to antibiotic resistance. But phage can also be used to treat infections that are completely resistant to antibiotics. In fact, a young cystic fibrosis patient who was fatally ill with an *M. abscessus* infection was successfully treated with a cocktail of genetically engineered phage, including BPs (Dedrick et al., 2019, Dedrick et al., 2019 (B)). Furthering our understanding of bacterial resistance mechanisms, including prophage, will provide insight into alternative therapeutics for antibiotic resistant infections, like phage therapy.

REFERENCES

Atsumi S and Little J. 2006. Role of the lytic repressor in prophage induction of phage ƛ as analyzed by a module-replacement approach. *PNAS*. 103(12):4558-4563). DOI: http://www.pnas.orgcgidoi10.1073pnas.0511117103/.

Barka et al., 2016. Taxonomy, physiology, and natural products of Actinobacteria. *Microbiol Mol Biol Rev*. 80:1–43. DOI:10.1128/MMBR.00019-15.

Bassler, B. 1999. How bacteria talk to each other: regulation of gene expression by quorum sensing. *Curr Opin Microbiol*. 2: 582-587.

Beck, H., Moll, I. 2018. Leaderless mRNAs in the Spotlight: Ancient but Not Outdated! *Microbiol. Spec*. 6(4): RWR-0016-2017. DOI: 10.1128/microbiolspec.RWR-0016-2017.

Bharati, B., Chatterji, D. 2013. Quorum sensing and pathogenesis: role of small signaling molecules in bacterial persistence. *Current Science*. 105(5): 643-656.

Broussard et al., 2013. Integration-dependent bacteriophage immunity provides insights into the evolution of genetic switches. *Mol Cell*. 49(2): 237-248. DOI: 10.1016/j.molcel.2012.11.012.

Brussow et al., 2004. Phages and the Evolution of Bacterial Pathogens: from Genomic Rearrangements to Lysogenic Conversion. *Microbiol Mol Biol Rev*. 68(3):560-602.

Bryant et al., 2013. Whole-genome sequencing to identify transmission of *Mycobacterium abscessus* between patients with cystic fibrosis: a retrospective cohort study. *The Lancet*. 381(9877): 1551-1560. DOI: https://doi.org/10.1016/S0140-6736(13)60632-7.

Burian et al., 2012. (B). The Mycobacterial Transcriptional Regulator *whiB7* Gene Links Redox Homeostasis and Intrinsic Antibiotic Resistance. *J Biol Chem*. 287(1): 299-310. DOI: 10.1074/jbc.M111.302588.

Burian et al., 2012. WhiB7, a transcriptional activator that coordinates physiology with intrinsic drug resistance in Mycobacterium tuberculosis. *Expert Rev. Anti Infect. Ther. 10*(9): 1037-1047. DOI: 10.1586/eri.12.90.

Burian, 2018. Regulatory genes coordinating antibiotic-induced changes in promoter activity and early transcriptional termination of the mycobacterial intrinsic resistance gene *whiB7*. *Mol Microbiol*. 107(3):402-415. DOI: https://doi.org/10.1111/mmi.13890.

Bussi, C., Gutierrez, MG. 2019. *Mycobacterium tuberculosis* infection of host cells in space and time. *FEMS Microbiol Rev*. 43(4): 341-361. DOI: 10.1093/femsre/fuz006.

Caratenuto et al., 2019. Genome Sequences of Six Cluster N Mycobacteriophages, Kevin1, Nenae, Parmesanjohn, ShrimpFriedEgg, Smurph, and SpongeBob, Isolated on Mycobacterium smegmatis mc2155. *Microbiol Resour Announc*. 8: e00399-19. DOI: 10.1128/MRA.00399-19.

Cresawn et al. 2011. Phamerator: a bioinformatics tool for comparative bacteriophage genomics. *BMC Bioinformatics*. 12:395. DOI: 10.1186/1471-2105-12-395.

Cresawn et al. 2015. Comparative Genomics of Cluster O Mycobacteriophages. *PLoS ONE*. 10(3): e0118725. DOI: 10.1371/journal.pone.0118725.

Daley, C., Griffith, D. 2016. Murray and Nadel's Textbook of Respiratory Medicine. *Nontuberculosis Mycobacterial Infections*.1:629-645. DOI: https://doi.org/10.1016/B978-1-4557-3383-5.00036-1.

De Moura et al., 2012. Gene Replacement in *Mycobacterium chelonae*: Application to the Construction of Porin Knock-Out Mutants. *PLoS One*. 9(4): e94951. DOI: 10.1371/journal.pone.0094951.

Dedrick et al., 2013. Functional requirements for bacteriophage growth: gene essentiality and expression in mycobacteriophage Giles. *Mol. Microbiol*. 88(3): 577-589. DOI: 1111/mmi.12210.

Dedrick et al., 2016. Function, expression, specificity, diversity, and incompatibility of actinobacteriophage *parABS* systems. *Mol Microbiol*. 101(4): 625-644. DOI: 10.1111/mmi.13414.

Dedrick et al., 2017. Prophage-mediated defense against viral attack and viral counter-defense. *Nat Microbiol*. DOI: 10.1038/nmicrobiol.2016.251.

Dedrick et al., 2019. (B). Mycobacteriophage ZoeJ: A broad host-range close relative of Mycobacteriophage TM4. *Nat Med*. 25(5): 730-733. DOI: 10.1038/s41591-019-0437-z.

Dedrick et al., 2019. Mycobacteriophage ZoeJ: A broad host-range close relative of Mycobacteriophage TM4. *PLoS One*. 10(9): e0137187. DOI: 10.1371/journal.pone.0137187.

Fan et al., 2016. Distribution and function of prophage phiRv1 and phiRv2 among Mycobacterium tuberculosis complex. *J Biomol Struct Dyn*. 34(2):233-238

Fang et al., 2017. Induction of Shiga Toxin-Encoding Prophage by Abiotic Environmental Stress in Food. *Appl Environ Microbiol* 83(19):1-13. Doi: https://doi.org/10.1128/AEM .01378-17.

Fibriansah et al. 2012. Crystal Structures of Two Transcriptional Regulators from *Bacillus cereus* Define the Conserved Structural Features of a PadR Subfamily. *PLoS One*. DOI: 10.1371.journal.pone.0048015.

Flentie et al. 2016. *Mycobacterium tuberculosis* transcription machinery: ready to respond to host attacks. *J Bacteriol*. 198: 1360-1373. DOI: 10.1128/JB.00935-15.

Gao et al., 2013. Purification of bacteriophage lambda repressor. *Protein Expr Purif*. 91(1): 30-36. DOI: 10.1016/j.pep.2013.06.013.

Gibson et al. 2009. Enzymatic assembly of DNA molecules up to several hundred kilobases. *Nat Methods*. 6(5): 343-345. DOI: 10.1038/nmeth.1318.

Grindley et al., 2006. Mechanisms of Site-Specific Recombination. *Annu. Rev. Biochem.* 75: 567-605. DOI: 10.1146/annurev.biochem.73.011303.073908.

Groth, A., Calos, M. Phage Integrases: Biology and Applications. 2004. *J. Mol. Biol.* 335:667-678.

Hatfull et al., 2010. Comparative genomic analysis of sixty mycobacteriophage genomes: Genome clustering, gene acquisition and gene size. *J Mol Biol.* 397(1): 119-143. DOI: 10.1016/j.jmb.2010.01.011.

Hatfull, 2011. Bacteriophages and their Genomes. *Curr Opin Virol*. 1(4):298-303.

Hatfull, 2014. Molecular Genetics of Mycobacteriophages. *Microbiol Spectrum*. 2(2):1-36.

Hatfull, 2018. Mycobacteriophages. *Microbiol Spectr*. 6(5). DOI: 10.1128/microbiolspec.GPP3-0026-2018.

Hauf et al. 2019. PadR-type repressors controlling production of a non-canonical FtsW/RodA homologue and other trans-membrane proteins. *Sci. Rep*. 9: 10023. DOI: 10.1038/s41598-019-46347-w.

Hendrix, 2003. Bacteriophage genomics. *Curr Opin Microbiol*. 6(5): 506-11. DOI: 10.1016/j.mib.2003.09.004.

Hess, K., Rudra, P., Ghosh, P. 2017. Mycobacterium abscessus WhiB7 Regulates a Species-Specific Repertoire of Genes To Confer Extreme Antibiotic Resistance. *Antimicrob Agents Chemother*. 61(1): 1-11. DOI: 10.1128/AAC.01347-17.

Holliday. 1964. A mechanism of gene conversion in fungi. *Genet Res Camb*. 5: 282-304. DOI: 10.1017/S0016672300001233.

Jacobs-Sera et al., 2012. On the nature of mycobacteriophage diversity and host preference. *Virology*. 434(2): 187-201. DOI: 10.1016/j.virol.2012.09.026.

Jones et al., 2019. Current Significance of the *Mycobacterium chelonae-abscessus* group. *Diagn Microbiol Infect Dis*. 94:248-254. doi: 10.1016/j.diagmicrobio.2019.01.021

Jones, B., Sall, J. JMP statistical discovery software. 2011. *WIREs Comp Stat.* 3: 188-194. DOI: 10.1002/wics.162.

Klumpp, S., Hwa, T. 2014. Bacterial growth: global effects on gene expression, growth feedback and proteome partition. *Curr Opin Biotechnol*. 0: 96-102. DOI: 10.1016/j.copbio.2014.01.001.

Kumari et al., 2018. Structural and functional characterization of the transcriptional regulator Rv3488 of Mycobacterium tuberculosis H37Rv. *Portland Press*. 475:3393-3416. DOI: 10.1042/BCJ20180356.

Lee et al., 1991. Site-specific integration of mycobacteriophage L5: Integration-proficient vectors for *Mycobacterium smegmatis*, *Mycobacterium tuberculosis*, and bacille Calmette-Guérin. *Prc. Natl. Acad. Sci. USA*. 88:3111-3115. DOI: 10.1073/pnas.88.8.3111.

Lee et al., Mycobacterium abscessus complex infections in humans. 2015. *CDC*. 21(9):1638-1646. DOI: http://dx.doi.org/10.3201/eid2109.141634

Livak KJ, Schmittgen TD. 2001. Analysis of relative gene expression data using real-time quantitative PCR and the 2(-Delta Delta C(T)) Method. Methods. 25(4):402-8. DOI: 10.1006/meth.2001.1262.

MacNeil et al., 2019. Global Epidemiology of Tuberculosis and Progress Toward Achieving Global Targets — 2017. *MMWR Morb Mortal Wkly Rep*. 68:263–266. DOI: http://dx.doi.org/10.15585/mmwr.mm6811a3.

McFee. 2013. Mycobacterium chelonae. *Disease-a-Month*. 59:439-440. DOI: https://doi.org/10.1016/j.disamonth.2013.10.007.

Nanda, A., Thormann, K., Frunzke, J. 2015. Impact of Spontaneous Prophage Induction on the Fitness of Bacterial Populations and Host-Microbe Interactions. *J Bacteriol*. 197(3): 410-419. DOI: 10.1128/JB.02230-14.

Nyugen, L. and Thompson, C. 2006. Foundations of antibiotic resistance in bacterial physiology: the mycobacterial paradigm. *TRENDS in Microbiology*. 14(7): 304-312. DOI: 10.1016/j.tim.2006.05.005.

Park et al., 2017. Structural basis of effector and operator recognition by phenolic acid-responsive transcriptional regulator PadR. *Nucleic Acids Res*. 45(22):13080-13093. DOI: 10.1093/nar/gkx1055.

Percival, S., Williams, D. 2014. Microbiology of Waterborne Diseases (Second Edition). *Mycobacterium*. 177-207. DOI: https://doi.org/10.1016/B978-0-12-415846-7.00009-3.

Petrova, Z., Broussard, G., Hatfull, G. 2015. Mycobacteriophage-repressor-mediated immunity as a selectable genetic marker: Adephagia and BPs repressor selection. *Microbiol*. 161(8): 1539-1551. DOI: 10.1099/mic.0.000120.

Pope et al. 2011. Expanding the Diversity of Mycobacteriophages: Insights into Genome Architecture and Evolution. *PLoS ONE*. 6(1): e16329. DOI: 10.1371/journal.pone.0016329.

Pope et al., 2017. Bacteriophages of *Gordonia* spp. Display a Spectrum of Diversity and Genetic Relationships. *mBio*. 8(4): e0169-17. DOI: 10.1128/mBio.01069-17.

Rokney et al., 2008. Host responses influence on the induction of lambda prophage. *Mol Microbiol*. 68(1): 29-36. DOI: 10.1111/j.1365-2958.2008.06119.x.

Russell D, Hatfull G. 2017. PhagesDB: the actinobacteriophage database. *Bioinformatics*. 33(5): 784-786. DOI: https://doi.org/10.1093/bioinformatics/btw711.

Sampson et al., 2009. Mycobacteriophages BPs, Angel and Halo: comparative genomics reveals a novel class of ultra-small mobile genetic elements. *Microbiology*. 155:2962-2977. DOI: 10.1099/mic.0.030486-0.

Schwartz et al., 2018. Against Multidrug-Resistant Nontuberculous Mycobacteria Recovered from Patients with Cystic Fibrosis. *Microbial Drug Resistance*. 24(8):1191-1197. DOI: 10.1089/mdr.2017.0286.

Shell et al. 2015. Leaderless Transcripts and Small Are Common Features of the Mycobacterial Translational Landscape. *PLoS*. 11(11): e1005641. DOI: 10.1371/journal.pgen.1005641.

Shimatake, H., Rosenberg, M. 1981. Purified ƛ regulatory protein cII positively activates promoters for lysogenic development. *Nature*. 292: 128-132. DOI: 10.1038/292128a0.

The World Health Organization (WHO). 2019. *Global Tuberculosis Report*.

Untergasser et al., 2012. Primer3-new capabilities and interfaces. *Nucleic acids res*. 40(15):e115. DOI: 10.1093/nar/gks596.

Vatlin et al. 2018. A functional study of the global transcriptional regulator PadR from a strain *Streptomyces fradiae*-nitR+bld, resistant to nitrone-oligomycin. *J Basic Microbiol.* 58: 739-746. DOI: 10.1002.jobm.201800095.

Villanueva V, Oldfield L, Hatfull G. 2015. *An Unusual Phage Repressor Encoded by Mycobacteriophage BP*s. *PLoS ONE*. 10(9):1-21. DOI: 10.1371/journal.pone.0137187.

Wang et al., 2010. Cryptic prophages help bacteria cope with adverse environments. *Nat. Commun.* 1(9):147-149. DOI: 10.1038/ncomms1146.

Zaman. 2010. Tuberculosis: A Global Health Problem. *J Health Popul Nutr*. 28(2): 111-113. DOI: 10.3329/jhpn.v28i2.4879.

Zaunbrecher et al. 2009. Overexpression of the chromosomally encoded aminoglycoside acetyltransferase *eis* confers kanamycin resistance in *Mycobacterium tuberculosis*. *PNAS*. 106(47): 200004-20009. DOI: 10.1073/pnas.0907925106.

Zhao et al. 2020. Quorum-Sensing Regulation of Antimicorbial Resistance in Bacteria. *Microorganisms*. 8(3): 425.

Zimmermann et al. 2018. A Completely Reimplemented MPI Bioinformatics Toolkit with a New HHpred Server at its Core. *J Mol Biol*. S0022-2836(17): 30587-9.

BIOGRAPHY OF THE AUTHOR

Emma Denise Freeman was born in Bangor, Maine and raised in Scarborough, Maine. She graduated from Scarborough High School in 2016. She will graduate from the University of Maine with a B.S. in Microbiology and a minor in Psychology. During her time at the University of Maine, Emma was a member of the All Maine Women honor society, served as the president of Operation H.E.A.R.T.S., volunteered with Partners for World Health, and served on the Black BearTHON committee. After graduation, she hopes to pursue a degree in medicine and one day return to Maine as an obstetrician or neonatologist.